OPEN ACCESS Freely available online

Journal of Geography & Natural Disasters

Research Article

High Obliquity, High Angular Momentum Earth as Moon's Origin Revisited by Advanced Kinematic Model of Earth-Moon System

Bijay Kumar Sharma*

Department of Electronics and Communication, National Institute of Technology, Patna, Bihar, India, 800005

APPENDIX A

A 1.1: Evolution of inclination of lunar orbital plane, eccentricity of lunar orbit and obliquity of Moon's spin axis based on the information in Cuk et.al

A 1.1.1: Evolution of Moon's orbital plane inclination angle (α) from 30 R_E (Cassini State Transition orbit) to 60 R_E (current lunar orbit) based on Cuk et.al. in Table A1.1. Gives the evolution of inclination angle:

The approximate FIT to the ListPlot in Figure A1.1 and Figure A 1.2 [1].

Inclination angle α =

$$1.18751\times10^{\wedge}25/a^{\wedge}3-7.1812\times10^{\wedge}16/a^{\wedge}2+1.44103\times10^{\wedge}8/a-8.250567342\times10^{\wedge}-3 \quad \ldots\ldots A1.1$$

Figure A 1.3 gives the correspondence between the List Plot and (A 1.1). The correspondence is good hence (A 1.1) gives the evolutionary history of Moon's orbital plane inclination angle in radians.

Table A1.1: Evolution of inclination angle (α) from 30 R_E to 60.336 R_E.

'a'(× R_E)	'a'(× 10^8 m)	α (°)	α (radians)
30	1.9113	28	0.4887
35	2.22985	16	0.279
40	2.5484	9.2	0.16057
45	2.86695	8	0.1396
50	3.1855	7	0.122
55	3.50405	6	0.1047
60	3.8226		
60.336	3.844	5.14	0.0897

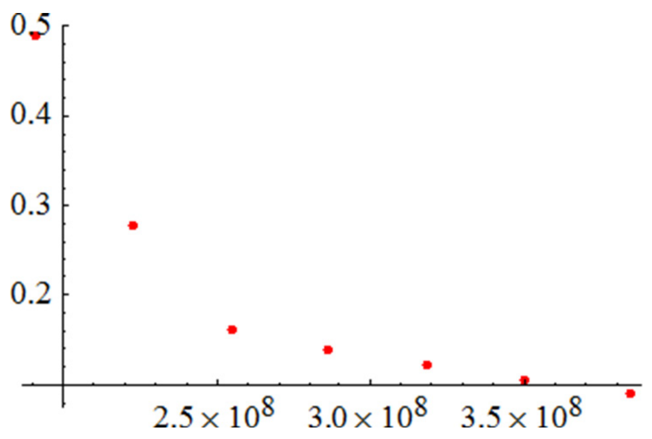

Figure A1.1: List Plot of the inclination angles in Table A1.1.

A 1.2: Evolution of Moon's Obliquity angle which currently is β =1.54°

Evolution of Moon's Obliquity angle (β) from 30 R_E (Cassini State Transition orbit) to 60 R_E (current lunar orbit) based on Cuk et.al [1].

Table A 1.2. gives the evolution of Moon's Obliquity angle

Table A1.2: Evolution of Moon's Obliquity angle (β) from 30 R_E to 60.336 R_E.

'a'(× R_E)	'a'(× 10^8 m)	β (°)	β (radians)
30	1.9113	70	1.22
35	2.22985	55	0.96
40	2.5484	40	0.698
45	2.86695	29.27	0.5109
50	3.1855	19.25	0.336

Correspondence to: Bijay Kumar Sharma, Department of Electronics and Communication, National Institute of Technology, Patna, Bihar, India, 800005, Tel: +919334202848; E-mail: bksharma@nitp.ac.in

Received: 10-Jul-2023, Manuscript No. JGND-23-20005; **Editor assigned:** 13-Jul-2023, PreQC No. JGND-23-20005 (PQ); **Reviewed:** 31-Jul-2023, QC No. JGND-23-20005; **Revised:** 07-Aug-2023, Manuscript No. JGND-23-20005 (R); **Published:** 14-Aug-2023, DOI: 10.35841/2167-0587.23.13.282

Citation: Sharma BK (2023) High Obliquity, High Angular Momentum Earth as Moon's Origin Revisited by Advanced Kinematic Model of Earth-Moon System. J Geogr Nat Disasters. 13: 282

55	3.50405	9.27	0.1618
60.336	3.844	1.54	0.0269
0.1396	0.1396	0.1396	0.1396

The approximate FIT to the ListPlot in Figure A 1.4. is:

$$Moon's\ Obliquity\ angle\ \beta = 3.36402 - 1.37638\times10^{-8}.a + 1.32216\times10^{-17}a^2 \ldots (A1.2)$$

Plot of (A 1.2) is as follows as shown in Figure A 1.5 and Figure A 1.6

The correspondence is good hence (A 1.2) gives the evolutionary history of Moon's Obliquity angle in radians.

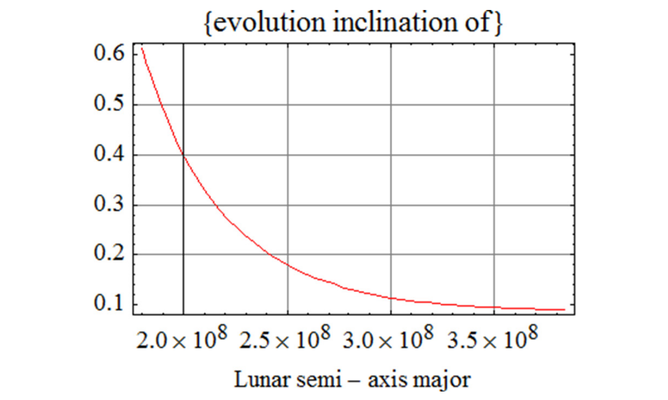

Figure A1.2: Plot of the FIT function (A1.1).

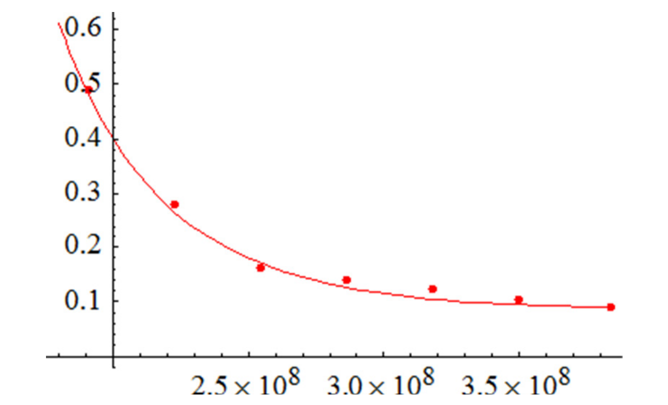

Figure A1.3: The superposition of the List Plot and the FIT Plot.

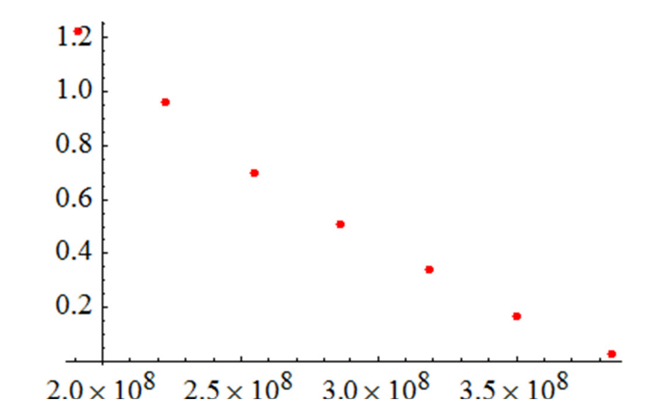

Figure A1.4: List Plot of the Moon's Obliquity angles given in Table A1.2.

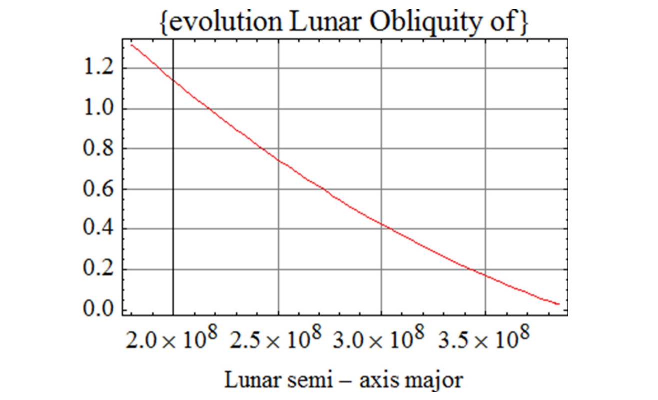

Figure A1.5: Plot of the FIT function (A1.2).

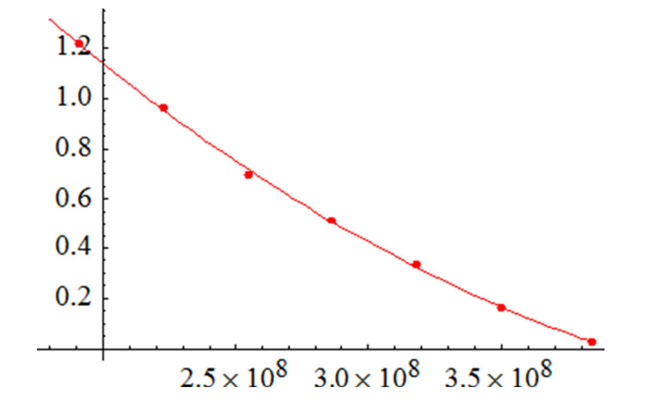

Figure A1.6: Superposition of List Plot and Fit Plot of Moon's Obliquity angle.

A 1.3: Evolution of Moon's orbit's eccentricity (e)

About 80% higher Angular Momentum (AM) E-M system with highly tilted Earth was born after being impacted by Theia. The Moon accreted from the glancing angle impact generated well mixed Earth's mantle and impactors debris. As fully formed Moon spiraled outward it passed through Laplace Plane Transition (r_L) at 17 R_E. The passage through (r_L) in highly oblique Earth's environment excited high eccentricity in Moon's orbit and high inclination of Moon's Orbital Plane. High eccentricity drained the excess AM to heliocentric Earth's orbit and Moon's orbit was circularized through Earth and Moon tidal interaction. Hence highly eccentric orbit excited by Laplace Plane transition was eventually circularized and synchronized. Table A 1.3 gives the evolution of Lunar Orbit's eccentricity (e) from a=30 R_E to 60.336 R_E.

ListPlot of the Moon's eccentricity given in Table A 1.3.

Table A1.3: Evolution of Moon's orbit eccentricity from 30 R_E to 60.336 R_E.

'a'(× R_E)	'a'(× 10^8 m)	e
30	1.9113	0.25
35	2.22985	0.23
40	2.5484	0.21
45	2.86695	0.2

50	3.1855	0.15
55	3.50405	0.1
60.336	3.844	0.0549

The approximate FIT to the ListPlot in Figure A 1.7 is:

$$e = 0.210252 + 8.38285\times10^{-10} a - 3.23212\times10^{-18} a^2 \quad \ldots\ldots (A1.3)$$

The Plot of (A 1.3) is as follows as shown in Figure A 1.7

Plot of Fit Function (A 1.3) as shown in Figure A 1.8

Superposition of eccentricity ListPlot and Fit Plot is given in Figure A 1.9.

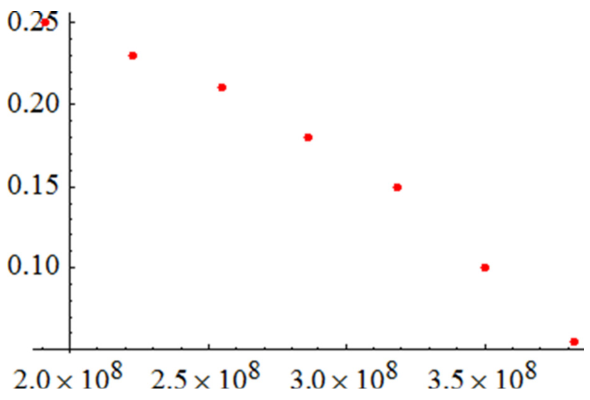

Figure A1.7: List Plot of the Moon's eccentricity given in Table A1.3.

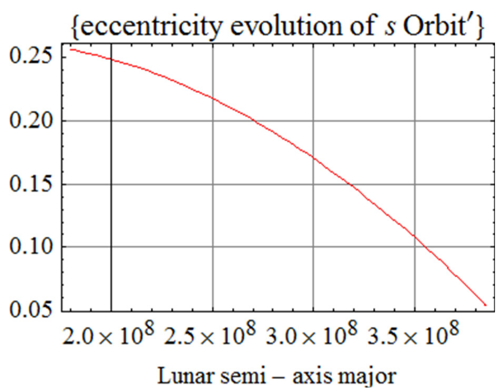

Figure A1.8: Plot of Fit Function (A1.3).

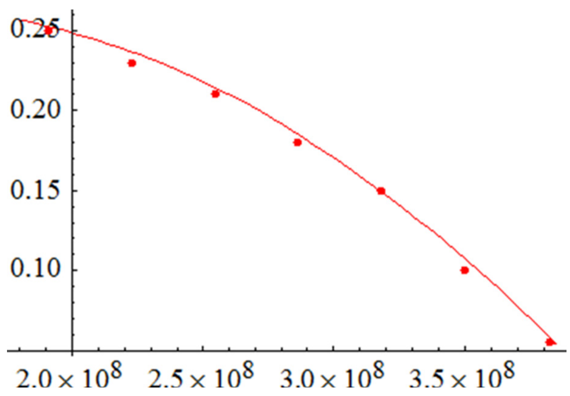

Figure A1.9: Superposition of List Plot and Plot of Moon's orbit eccentricity A1.3.

The correspondence is good hence (A 1.3) gives the evolutionary history of Moon's Orbit eccentricity.

A 1.4: The determination of the evolutionary history of Earth's Obliquity from advanced kinematic model of tidally interacting E-M system

From a previous personal communication arXiv: http://arXiv.org/abs/0805.0100

LOM/LOD of Earth Moon system is known over the past geologic epochs.

$$LOM/LOD = (1/C)\left[T\times a^{2}/(Y\times B) - D - M\times a^{2}\right]$$

Where $D = 8.878598241\times10^{34}\,Kg-m^{2}$,

$(\text{reduced mass of Moon}) = 7.258980539\times10^{22}\,Kg$,

$JT = 3.44048888\times10^{34}(Kg-m^{2})/s$

$Y = (a^{12} - A\times a^{(5/2)} + A\times a72Z)$

$A = 9.14257051\times10^{-22^{-2}}m^{-2}$

$Z = 5.52887891\times10^{8}m$

$B = 2.008433303\times10^{7}m3/2/$

$C = 8.02\times10^{37}(Kg-m^{2})$;... A 1.4 LOM/LOD for various geological epochs are tabulated in Table A 1.4.

Table A1.4: LOM/LOD and Earth's Obliquity for past geological epochs.

a(× R_E)	a(× 10^8 m)	LOM/ LOD	Sin [θ]	(radians)	θ°°
30	1.9	23.3752	-0.464076	unstable	unstable
35	2.23	26.1194	-0.216896	unstable	unstable
40	2.5484	28.1147	0.0213757	0.0213773	1.22483
45	2.867	29.2938	0.113547	0.113792	6.51
50	3.1855	29.5965	0.218451	0.220227	12.6
55	3.5	28.9877	0.309749	0.314929	18
60	3.82	27.4	0.388198	0.398676	22.84
60.335897	3.844	27.32	0.397788	0.409105	23.44
3.844	3.844	3.844	3.844	3.844	3.844

As Moon's orbital plane gets damped from 27.54 degree to 5.14 degree under the influence of strong lunar obliquity tides, Earth's obliquity increases from 1.22483 degree to 23.44 degree.

Rewriting (23) from main Text:

$$(N)^{2}\times a^{3} = X^{2} + (F\sqrt{(1-k^{2})})^{2}\times(a^{2})^{2} + G^{2} + 2(F\sqrt{(1-k^{2})}\times a^{2})(G)\{\sqrt{(1-D^{2})}\sqrt{(1-A^{2})} - AD\} + 2\times X\times\sqrt{(F(\sqrt{(1-k^{2})}\times a^{2})^{2} + (G)^{2} + 2((F\sqrt{(1-k^{2}\times a^{2})}(G)\{\sqrt{(1-D^{2})}\sqrt{(1-A^{2})} - AD\}\times\{\sqrt{(1-A^{2})}\sqrt{(1-B^{2})} - A.B\}$$

... $A1.5$

In (A 1.5) all constant and all spatial functions are known except the obliquity angle ϕ. For a given lunar orbit, X=LOM/LOD is known. Using this information Sin [ϕ] is determined and hence ϕ and tabulated in Table A 1.4

We have six set of data from a=30 R_E to the present day semi-major axis.

We clearly see that at Cassini State Transition i.e. at 33 R_E, obliquity is indeterminate. From 45 R_E to 60.336 R_E obliquity is well behaved and it is increasing. It increases from 6.51° to 23.44°. This means that during angular momentum conservative phase i.e. from Cassini State Transition to the present epoch, reduction in Moon's plane inclination is accompanied with increase in obliquity by necessity.

A 1.4.1. Evolutionary spatial functions of terrestrial obliquity (ϕ) and LOM/LOD

Evolutionary spatial functions of inclination angle (α), Moon's obliquity (β) and of eccentricity 'e' have been determined in CELE-D-17-00144 and given above. They are as follows:

Inclination angle α =

$1.18751\times10^{\wedge}25/a^{\wedge}3-7.1812\times10^{\wedge}16/a^{\wedge}2+1.44103\times10^{\wedge}8/a-8.250567342\times10^{\wedge}-3$

.... $A1.1$

Moon's obliquity angle $\beta=$
$3.36402-1.37638\times10^{\wedge}-8a+1.32216\times10^{\wedge}-17a^{\wedge}2$ A1.2

$e=0.210252+8.38285\times10^{\wedge}-10a-3.23212\times10^{\wedge}-18a^{\wedge}2$ ... $A1.3$ The LOM/LOD and Earth's obliquity angles are tabulated in Table A 1.4.

A 1.4.1.1. Evolutionary function of LOM/LOD: The approximate FIT function to the ListPlot of LOM/LOD in Table A 1.4. is:

$LOM\ /LOD=\omega/\Omega=-12.0501+2.6677\times10^{\wedge}-7\times a-4.27538\times10^{\wedge}-16\times a^{\wedge}2$ ...... $A1.6$ the plot of (A 1.6) is as follows shown in Figure A 1.10 and Figure A 1.11.

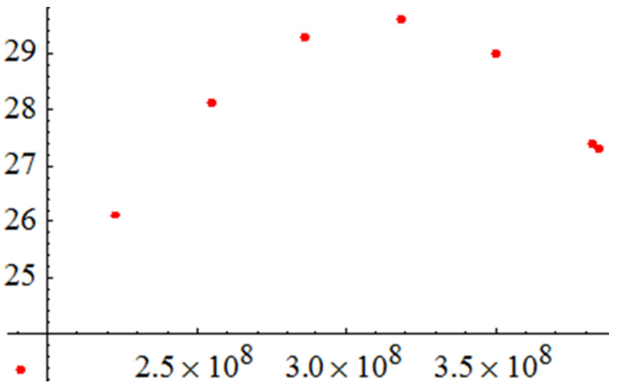

Figure A1.10: List Plot of LOM/LOD in different geologic epochs as given in Table A1.4.

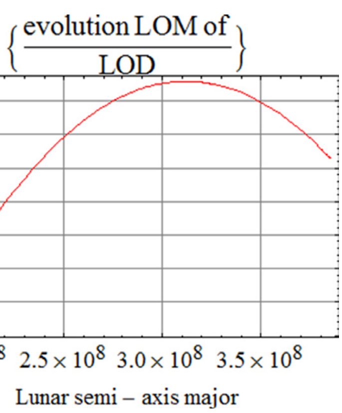

Figure A1.11: Plot of FIT function given by (A1.6).

Superposition of LOM/LOD ListPlot and Fit Plot is given in Figure A 1.12.

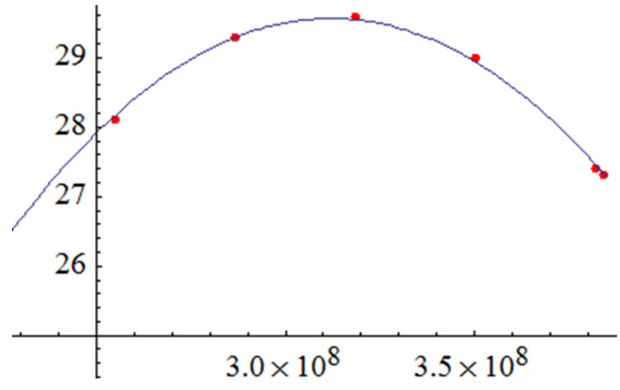

Figure A1.12: Superposition of LOM/LOD ListPlot and FIT Plot.

The correspondence between LISTPLOT and FIT PLOT is good hence (A 1.6) gives the evolutionary history of LOM/LOD.

A 1.4.1.2. Evolutionary function of Earth's obliquity: The approximate FIT function to the ListPlot of Earth's obliquity in Figure A 1.16 is: $\phi=-0.732299+2.97166\times10^{\wedge}-9\times a$ .... A1.7.

The Plot of (A 1.7) is as follows shown in Figure A 1.13 and Figure A 1.14.

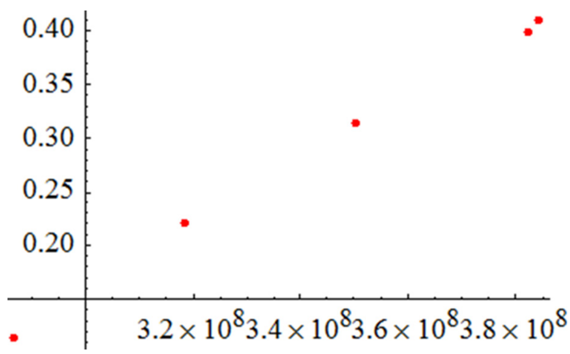

Figure A1.13: List Plot of Earth's obliquity (Φ) angle over different geological epochs given in Table A1.4.

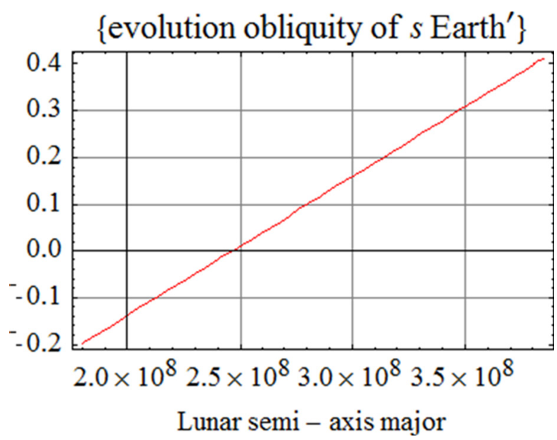

Figure A1.14: Plot of FIT function given by (A1.7).

Superposition of ListPlot and Fit function is given in Figure A 1.15.

The correspondence between LISTPLOT and FIT PLOT is good hence (A 1.7) gives an accurate evolutionary history of Earth's obliquity.

We have altogether 5 spatial function (A 1.1), (A 1.2), (A 1.3), (A 1.6) and (A 1.7) describing the evolution of inclination angle (α), Moon's obliquity (β), eccentricity (e) of lunar orbit, LOM/LOD and Earth's obliquity (ϕ) respectively through different geologic epochs. These are tabulated in Table A 1.5.

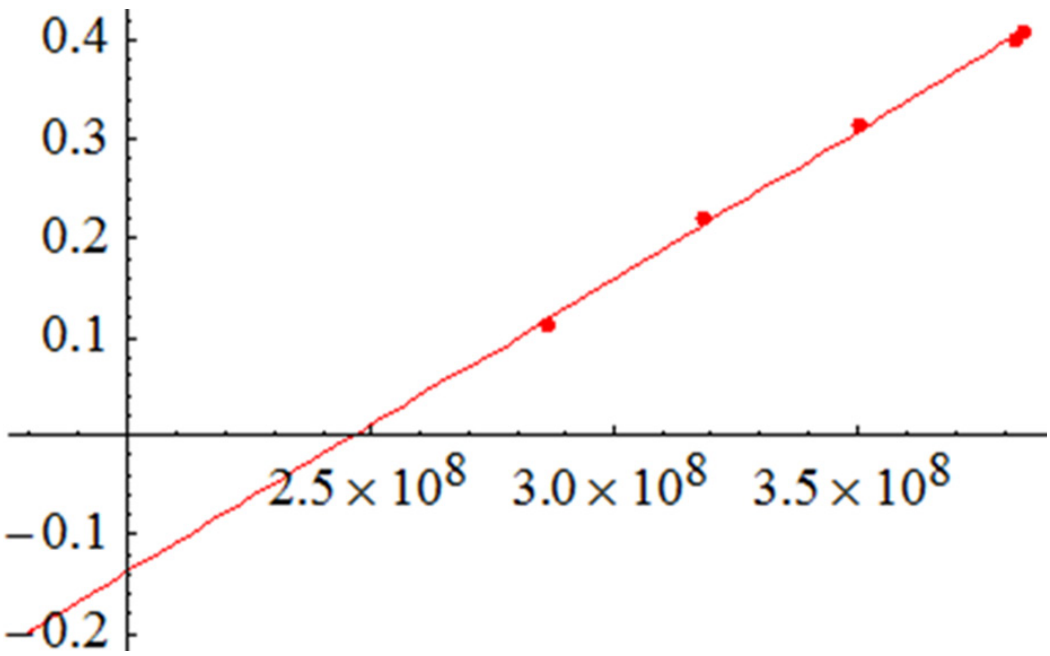

Figure A1.15: Superposition of List Plot of Earth's obliquity (Φ) and Fit Plot.

Table A1.5: Evolutionary history of ω/Ω (LOM/LOD), α (Inclination angle), β (lunar obliquity), e (eccentricity) and ϕ (terrestrial obliquity).

a (× R_E)	a (×108m)	ω/Ω	α radians	β radians	e	ϕ (rad)	Sin [ϕ]
30	1.9113	23.3752	0.480685 (27.4°)	1.21635 (69.69°)	0.2524	unstable	-0.464076
35	2.22985	26.1194	0.26478 (15.17°)	0.952317 (54.56°)	0.236	unstable	-0.216896
40	2.5484	28.1147	0.168969 (9.68°)	0.71512 (40.97°)	0.214	0.0213773	0.0123757
45	2.86695	29.2938	0.124631 (7.1408°)	0.504756 (28.92°)	0.1849	0.113792 (6.51°)	0.113547
50	3.1855	29.5965	0.103801 (5.04736°)	0.321225 (18.4°)	0.1493	0.220227 (12.6°)	0.218451
55	3.50405	28.9877	0.0941394 (5.39379°)	0.164527 (9.4267°)	0.10714	0.314929 (18°)	0.309749
60	3.8226	27.4	0.0898729 (5.149°)	0.03466 (1.986°)	0.0584	0.398676 (22.84°)	0.388198
60.336	3.844	27.32	0.08971 (5.14°)	0.0268 (1.54°)	0.0549	0.409105 (23.44°)	0.397788

LLR measurement of 3.7 cm/y was resulting in too short an age of Moon (~3 Gy) which was contrary to the observed age of the rocks brought from Moon during Apollo Missions from 1969 to 1972 (curation/Lunar-NASA). These missions brought 382 Kg of lunar rock, core samples, pebbles, sand and dust from the Moon surface. It is estimated that Moon's crust formed 4.4 by ago. A team of scientist have studied Apollo 14 zircon fragments. They put the age of Moon at 4.51 by [2]. Matija Cuk, Douglas P Hamilton, Simon J. Lock, Sarah T Stewart [1] finally have resolved this conundrum. According to this research, from 3 R_E to 45 R_E, Moon does not have a smooth monotonic and spiral expansion. In fact it is bumpy. It is chaotic, gets stuck in resonances and comes out of the resonances and gets stalled and resumes its tidal evolution. In fact Moon takes 3.267 Gy to spirally expand from 3 R_E to 45 R_E in fits and stalled manner. From 45 R_E to 60.336 R_E, Moon smoothly coasts in 1.2 Gy. This accelerated spiral expansion in the on-going phase results in present day velocity of recession of 3.7 cm/y. As we see this consistency with LLR results resolves a long standing problem of mismatch between observed LOD curve and theoretical LOD curve. In this new E-M model, a precise match is obtained between the theory and observation. The series of papers in CELMEC VII and the main text have set the stage for Advanced KM to be established as a well-tested tool for further applications in Space Dynamics. I also envisage the application of this model in earth-quake predictions (see S7 in Supplementary file).

A2. The algorithm for calculating the transit time from an earlier orbit to a later one

$$(a)=2K/(m^*B)\times(\sqrt{a}/a\wedge Q)[X-1]\times 31.5569088\times 10\wedge 6m/y \quad \text{...... A2.1}$$

The value of the constants in Equation (A2.1) are as follows:

$(structure\,constant)=8.33269\times 10\wedge 42(N-m\wedge Q)$,

$Exponent\,Q=3.22684$,

$m^*=reduced\,mass\,of\,Moon=7.256742697\times 10\wedge 22Kg$.

$B=\sqrt{(G(M+m))}=2.008774813\times 10\wedge 42m\wedge 3/2/s$

$a=lunar\,semi-major\,axis$

The given value of K(structure constant) and Q (exponent of the structure factor) ensure the modern day recession velocity of Moon as 3.82 ± 0.07 cm/y as measured in the current Lunar Laser Ranging Experiments [3].

Equation (23) in the main text is a quadratic equation in X=LOM/LOD. Equation (23) is solved and two roots are obtained. One is negative and the other is positive. The positive root is retained. The value of lunar orbital inclination angle (α in radians) given in Equation (31), the value of Moon's obliquity angle (β in radians) given in Equation (32), the value of Moon's orbit eccentricity described in Equation (33) ,and function of terrestrial obliquity angle (ϕ in radians) are substituted in the expression of D and Z . This form of X is substituted in (A2.1).

(A2.1) is used for calculating the transit time from any earlier orbit to the present orbit $3.844\times 10\wedge 8m$

The transit time is given by the following time integral:

$$Transit\,time\,from\,a1\,to\,a2=\int 1/(a)\,da;a2\,a1 \quad \text{...... A2.2}$$

SUPPLEMENTARY INFORMATION

S1. BACK GROUND OF THIS PAPER

On 20th July 1994, the author received a NASA Press release that through Lunar Laser Ranging experiment it had been ascertained that our Moon had receded by 1 m in last twenty five years from 20th July 1969 to 20th July 1994 which gives the recession rate of 3.82 ± 0.07 cm/y [3]. This gave the author the second boundary condition for the second order ordinary linear differential equation which he had set for E-M tidally interacting system. The first boundary condition had been provided by George Howard Darwin 100 years earlier. He had calculated that Moon will finally lock-in with Earth at the outer Geo-Synchronous orbit in a 44 triple synchrony state where Earth's spin=Moon's spin=Orbital period=47days [4,5]. With these two boundary conditions the author was able to solve the differential equation and obtain a time integral which gave the age of Moon as 2.8 Gy and if the Author took the age of Moon as 4.467 Gy (as it should be taken) then the lunar recession rate of 2.4 cm/y is achieved. The rate of recession as measured by Lunar Laser Ranging experiment is anomalously high and leads to an Age of Moon (2.8 Gy) which is completely contradicted by the dated lunar Basalts along with paleontological and sedimentological data. It was only after Matija Cuk et al [1] published their paper that the Author was able to see that Earth-Moon tidal interaction has not been steady and monotonic. After Laplace Plane transition the tidal interaction was stalled and even reversed and Moon has evolved in Fits and Bound. Once this is taken care of, the zigsaw puzzle falls in its place and theoretical formalism of observed LOD provided by John West Wells [6,7], Kaula and Harris [8] and Charles P Sonett [9] exactly matches the observed LOD curve. It is correct that the present rate of tidal dissipation is anomalously high and this is because Moon is in accelerated tidally expanding spiral path. It is in an accelerated spiraling path because it lost time in halted tidal evolution at Laplace Plane Transition and at Cassini State transition. The first paper by the Author on Earth-Moon System was presented at 82nd Indian Science Congress [10]. This work was further expanded to arrive at the theoretical formalism of lengthening of day curve and matching it with the observed LOD curve obtained by John West Wells [6,7], Kaula and Harris [8] and Charles P Sonnett [9]. This was published in arXiv as a personal communication of the Author: http://arXiv.org/abs/0805.0100. In 2002 the author had discovered the dynamics of Earth-Moon tidally interacting pairs and the result was reported in World Space Congress held in Houston, Colorado, USA [11]. By this time the author realized that George Howard Darwin talked about the outer geosynchronous orbit only whereas in fact there was an inner geosynchronous orbit at 15,000 Km and Roche's Limit [12] of 18,000 Km fell beyond 15,000 Km and hence when Moon was fully formed it was by necessity in a super-synchronous orbit and by gravitational sling shot it was catapulted on an expanding spiral orbital path which we witness today by Lunar Laser Ranging (LLR) and we are recording a recession rate of 3.82 ± 0.07 cm/y by our Moon [3]. In 2004 the author found that Earth-Moon results could be generalized to any tidally interacting pairs and planet-satellite dynamics was extended to Sun-planets system and presented 3 papers at 35th COSPAR Scientific Assembly held in 2004 in Paris. In this Assembly the author presented a NEW PERSPECTIVE on solar and exo-solar systems

[13,14]. The author extended this to several exo-solar systems and presented it as The Architectural Design Rules of Solar System at CELMEC V in 2009 in Italy [15]. In 2012 the author presented the Paper No. B0.3-0011-12 at 39th Scientific Assembly-2012 [16]. The correspondence between Newtonian formalism of synchronous orbit and kinematic formalism of Clarke's orbit or synchronous orbit (Clarke's Orbit is geo-synchronous orbit in E-M system) was found and graphically illustrated for vanishingly small mass ratios. On 20th June 2016 the discovery of an infant planet has been reported [17]. The central tenant of the kinematic model is that planets are always born at inner Clarke's Orbit and from there they either get trapped in a collapsing death spiral as K2-33 b is trapped or they get launched on an expanding spiral orbit as our Moon is. K2-33 b gave us a rare opportunity to look at the birth orbit of the planets and it was exactly as predicted by kinematic model. The manuscript with the title "Birth Orbit of K2-33 b revealed by kinematic model of tidally interacting binaries" is under preparation. Mars moons Phobos and Deimos have also been born in the inner Clarke's orbit of M-P-D system [18,19]. Author's predictions made in 35th Scientific Assembly [13] are being confirmed by observational astronomy. All the planets - Giant first and terrestrial planets subsequently- are born at inner Clarke's Orbits as testified by IR imaging of the annular dark rings in circumstellar disc of many young stars [17] and also testified by meteoritic paleomagnetism measurements [20].

S2. KEPLERIAN ERA

The Kepler's Third Law for a given Planet-Sun configuration is:

$$a\,\hat{}3.\Omega\,\hat{}2=G(M+m) \quad \text{.... S2.1}$$

Equation (1) does not specify if the given orbital configuration is stable. Newton derived this law assuming that centripetal force (GMm/a^2)=centrifugal force ($\frac{mv_{Tang}^2}{a}$) where a=semi-major axis of Earth-Moon orbital configuration, M=mass of the Earth and m=mass of our Moon. By implication it was assumed that all configurations predicted by (1) are stable. By the end of 19th century George Howard Darwin put a question mark on this stability by publishing two papers on E-M system [4,5]. In 18th Century, German Philosopher Kant had suggested the theory of retardation of Earth's spin based on the ancient records of Solar Eclipses [21,22]. Similar kind of studies had been carried out by Kevin Pang at Jet propulsion Laboratory at Pasadena [23,24]. He happened to step upon certain ancient records regarding Solar Eclipses. A total Solar Eclipse had been observed in the town of Anyang, in Eastern China, on June 5, 1302 B.C. during the reign of Wu Ding. Had Earth maintained the present rate of spin, the Eclipse should have been observed in middle of Europe. This implies that in 1302 B.C. i.e. 3,291 years ago Earth's spin period was shorter by 0.047 seconds. This leads to a slowdown rate of 1.428 seconds per 100,000 years. In 1879 George Howard Darwin carried out a complete theoretical analysis of Earth-Moon System and put forward a sound hypothesis for explaining the slow down of Earth's spin on its axis. This marked the end of Keplerian Era. Gravitationally bound bodies were necessarily tidally interacting and tidal interaction led to tidal dissipation with inherent instability and hence a post Keplerian physics was required to deal with gravitationally bound binary pairs. Tidally dissipative system because of loss of energy cannot be stable. The system will evolve to a minimum energy state which is a stable configuration by necessity.

S3. THE BEGINNING OF EVOLUTIONIST VIEW OF UNIVERSE

By mid-20th century it was increasingly felt that just as electrons had radiation-less stable permissible orbits in exactly the same way celestial body pairs have two triple synchrony orbits (aG1 and aG2) where they are conservative systems and no dissipation of energy is involved [11,14,15]. Here triple synchrony orbits implies:

$$\omega(\textit{spin angular velocity of the primary})=\Omega(\textit{orbital angular velocity})=\Omega'(\textit{spin angular velocity of the secondary}$$

.... S3.1

The orbits of triple synchrony means geo-synchronous orbits in E-M system and Clarke's orbits in context of planet-satellite pairs, star-planet pairs, star-star pairs, Neutron Star- Neutron Star pairs (NS) pairs and NS and BH (black hole) pairs. Here planet-satellite pairs, star-planet pairs and star pairs are non-relativistic systems. NS pairs, NS and BH pairs or BH pairs are relativistic systems. Relativistic systems are radiating gravitational waves and they are being driven towards coalescence hence they are always unstable. But non-relativistic systems are stable at outer triple synchrony orbits. From George Howard Darwin's time it is recognized that planets raise body tides in their natural satellites and natural satellites raise body tides in their host planets. It is also recognized that planets and satellites are anelastic bodies (elastoviscous bodies). Hence tidal deformation (tidal stretching and squeezing) leads to dissipation of energy called tidal dissipation. This tidal dissipation causes mis-alignment of the tidal bulge and the radius vector of the secondary and the primary. Because of this mis-alignment an accelerating/or braking Tidal Torque is exerted on the primary body. By assuming different Love Numbers (kj) and different Q parameter, different rate of tidal dissipation can be incorporated in the tidal interaction. In Love Number, the subscript j is the harmonic degree, and kj is a proportionality constant, or Love number [25,26]. The Love numbers depend on internal structure of the deforming body, and reflect a competition between elastic and gravitational influences. If the elastic rigidity is sufficient, the body will deform very little, and the Love numbers will be near zero. If the gravitational effect dominates, the response will be purely hydrostatic. For a purely elastic body, the induced potential will be exactly aligned with the imposed potential, and there will be no torque, no dissipation, and no influence on the orbit. If there is dissipation, as would occur in a viscous or visco-elastic body, then the deformation (the tidal bulge) will lag behind the imposed potential in case of Sub-Synchronous Systems such as Mars-Phobos system and will lead the imposed potential in case of Super Synchronous Systems such as Earth-Moon. The rate of energy dissipation is proportional to the product of the stress times the strain rate, and will depend on the density, rigidity, viscosity, and rate of periodic forcing. From the tidal bulge lag angle, γ degree, the tidal torque as well as the Quality Factor can be determined. Quality Factor is the reciprocal of Tangent of tidal bulge lag angle which is taken as Q=85.58 for Mars and Tidal Torque is proportional to the product of Tidal Amplitude and Sin (γ degree). Tidal interaction occurs if the tidal bulge of the primary has an angle (leading or lagging) with the radius vector of the secondary component.

3.1. Spin down of the primary in super-synchronous

orbits

Tidal interaction inevitably leads to tidal drag (or secular deceleration) or spin down of the primary component if the satellite is long of synchronous orbit. Here the tidal bulge is leading the satellite's radius vector as in Earth-Moon (E-M) system. This is referred to as super-synchronous orbit as shown in Figure S3.1.

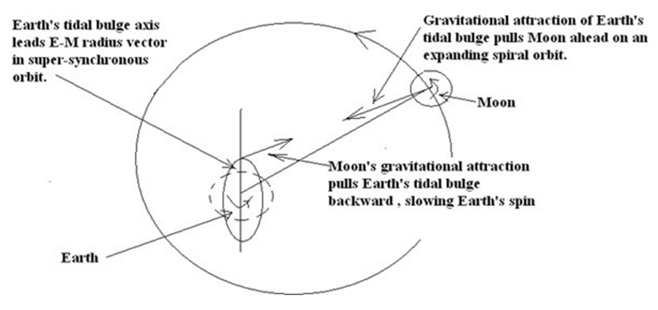

Figure S3.1: Earth's tidal bulge axis leads E-M radius vector in super synchronous orbit. This leads to tidal drag and de spinning of Earth leading to secular lengthening of solar day and gravitational attraction of Earth's tidal bulge pulls Moon ahead on an expanding spiral orbit.

3.2. Spin-up of the primary in sub-synchronous orbits

If the tidal bulge is lagging the radius vector of the secondary component then it is sub synchronous orbit. In this configuration tidal secular acceleration or spin-up of the primary component occurs as in Mars-Phobos (M-P) system as shown in Figure S3.2.

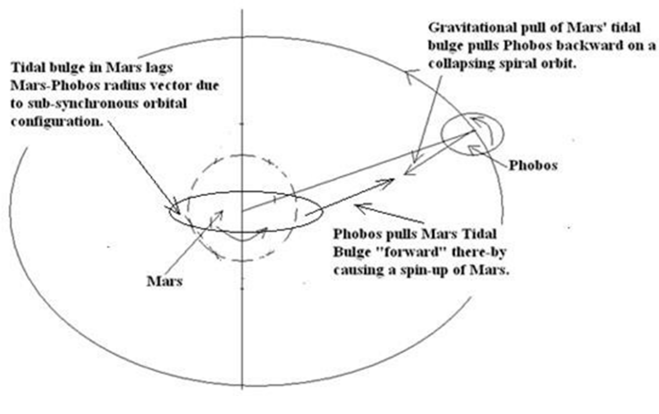

Figure S3.2: In Mars-Phobos System, Phobos is in sub-synchronous orbit. The tidal bulge in Mars lags M-P radius vector hence Phobos is spinning up Mars. Conservation of angular momentum causes Phobos to be launched on gravitational runaway collapsing spiral orbit also known as death spiral.

3.3. Lock-in at geo-synchronous orbits (aG1 and aG2)

It is zero tidal interaction if the two bodies are tidally interlocked. When the primary and secondary are tidally interlocked, the lag angle/lead angle become zero and the system is a conservative system. This is Triple Synchrony state as defined by (2) and it is called geosynchronous orbit in E-M system and it will be referred to as Clarke's orbits in all other binary pairs. As we will see all binary pairs have two Clarke's orbits, inner and outer Clarke's orbit. Inner Clarke's orbit is an equilibrium orbit but it is energy maxima hence unstable orbit. Outer Clarke's orbit is also an equilibrium orbit but energy minima and hence stable orbit [11,14,15]. A binary pair originates at inner Clarke's Orbit. Any perturbation such as solar wind, cosmic particles, star dust or radiation pressure perturbs the secondary component to a new orbit within or beyond aG1.

Figure S3.1 illustrates lead angle in E-M system and Figure S3.2. Illustrates the lag angle in M-P system. E-M system is in super-synchronous configuration that is Earth's tidal bulge leads Moon radius vector. Earth is experiencing a tidal brake by Moon and Moon is being pushed outward with a recession velocity of 3.82 (± 0.07) cm/y as established by Apollo Mission 11 initiated Laser Ranging Experiment [3]. Figure S3.2 illustrates that M-P is in sub synchronous configuration that is Mars' tidal bulge lags Phobos radius vector. Mars is being accelerated or spun-up by Phobos and Phobos is trapped in a death spiral i.e. it is traversing a collapsing spiral. In about 10 My to 20 My it is doomed to be tidally pulverized and spread like a ring around Mars just like Jupiter's or Saturn's ring [27]. In perfect tidal lock-in position, the long axis of the tidal bulge of primary and secondary components are exactly aligned and both the components orbit the barycenter as one single body as is the case with Pluto-Charon. This lock-in pair was video photographed by New Horizon. In NH Lorri OPNAV Campaign [13]. On 14th July 2015, Pluto-Charon were at the point of closest approach to New Horizon space probe and Pluto Charon were seen making circular paths around the barycenter which lay outside the two globes. The tidal stretching and squeezing completely stops and hence tidal dissipation is zero. This perfect lock-in occurs when the two components are synchronized, the orbit of each component around the barycenter are circularized and the orbital planes of the two components are co-planer. This observation in reference to stellar binaries had been made by Zahn [28-30].

"Eventually the Binary may settle in its state of minimum kinetic energy, in which the orbit is circular, rotation of both stars is synchronized with the orbital motion and the spin axis are perpendicular to the orbital plane. Whether the system actually reaches this state is determined by the strength of tidal interaction, thus by the separation of the two components, equivalently the orbital period. But it also depends on the efficiency of the physical process which are responsible for the dissipation of the kinetic energy."

Mars-Phobos is the example of sub-synchronous Satellite where Mars-Phobos Radius vector leads the tidal bulge in Mars [13], Phobos spins-up Mars and Phobos loses altitude. Mars spins-up because of transfer of angular momentum and orbital energy from Phobos to Mars. Earth-Moon is the example of super-synchronous Satellite where Earth-Moon Radius vector lags the tidal bulge in Earth, Moon is spinning down Earth (Earth's spin is slowing down at (2.3 ± 0.1) ms per century [31]. Earth was spinning at 5 h per day, today it is spinning at 23.9344 h per day and in its final lock-in orbit it will be spinning at 47 d per spin period) and Moon is receding at 3.82(± 0.07) cm/y presently [3]. Here angular momentum is being transferred from the Earth to our Moon. Pluto-Charon is the example of tidally interlocked orbital configuration where the tidal bulge of both the components are aligned and both the components are orbiting the barycenter as one body in a perfect circle [13,32] give the following tidal evolution equation:

$$a_{t=}[a_0^{13/2} - \frac{13}{2} \times \frac{3k_2}{Q}\sqrt{\frac{G}{M}} \times mR^5 \Delta t]^{2/13} \quad \text{...... S3.2}$$

Where k2 =Love Number of Mars,

Q is the quality factor,

M and R are the mass and radius of Mars, m=mass of Phobos, a0=current semi-major axis.

This equation gives the orbital radius=at at a time of Δt seconds ago.

In Equation (S3.2), Love Number and Quality Factor depend upon density, rigidity, viscosity and rate of periodic forcing. These parameters are known with large uncertainties for different Planets and their Satellites and hence their Tidal Evolutionary History will be arrived at with equal uncertainty in Seismic Model based analysis.

4. KINEMATIC MODEL OF E-M SYSTEM

As already noted in the last section, analysis of Seismic model requires the knowledge of a large number of material properties of the celestial objects which are known with a lot of uncertainties. Hence Author developed Kinematic Model of E-M system which required only the globe-orbit parameters and the age of E–M system. These are known with a high confidence level.

Assumptions of Kinematic Model:

E-M System is regarded as 3-body rotating system from its birth to its terminal point at the second geosynchronous orbit. The tidal drag of Sun for Lunar orbital radius greater than ten times Earth's radius is implicit in KM treatment. This is implicit in Advanced Kinematic Model (AKM) also (in the main text). (2) Total angular momentum of E-M System has been assumed to be the scalar sum of the orbital angular momentum of E-M system, spin angular momentum of Earth and spin angular momentum of Moon. For mathematical tractability this approximation is made. In the real world the obliquity angle (ϕ) or tilt angle of Earth's spin axis with respect to the Ecliptic plane normal, is 23.44^0, the inclination angle (α) of Moon's orbital plane with respect to the ecliptic plane is $\alpha = 5.14^0$ and axial tilt of Moon's spin axis with respect to Ecliptic Normal is β (Moon's Obliquity angle)=1.54^0 make the total angular momentum of E-M system (JTotal=J4) the vector sum of orbital angular momentum (J0), Moon's spin angular momentum (J1) and Earth's spin angular momentum (J2) . By making the above two assumptions the calculation becomes tractable but due to scalar summation serious errors are introduced. In the present paper an exact analysis is done by including the obliquity of Earth, orbital inclination of Moon and obliquity of Moon and by including the tidal drag of Sun at Laplace Plane transition and beyond, At 23-24 R_E Earth had become rigid enough to retain the oblateness it had acquired at that point and then onward the moment of inertia has remained constant at its modern value namely $C = 8.02\times10^{\wedge}37Kg - m2$. Hence evolving oblateness is not considered. Advanced Kinematic Model (AKM) considers the total angular momentum as the vectorial sum of Earth's spin angular momentum, Moon's spin angular momentum and orbital angular momentum of E-M system. After the semi-major axis reaches the Laplace Plane transition orbit namely a=17 R_E then solar perturbation comes into picture and it has to be accounted and it is implicit in AKM treatment Now we calculate the residual acceleration of Moon which according to Newton should be zero but is not zero and this precisely is the reason of instability outside geo-synchrony of E-M system:

$$Present\ centripetal\ acceleration = GM / a_{present}^2 = 2.69756\times10-3m/s^{\wedge}2 \quad \text{... . S4.1}$$

$$Present\ centrifugal\ accleration = \Omega_L^2 \times a_{present} \times \frac{1}{1+m/M} = 2.69026\times10-3m/s^{\wedge}2 \quad \text{..... S4.2}$$

Moon is effectively undergoing a radial deceleration of 0.0073 ẋ 10^-3 m/sec2. Its outward radial velocity is being decelerated until it becomes zero at the outer geo-synchronous orbit where it is in a triple synchrony state as shown in Figure S4.1: $\omega = \Omega = \Omega' = 2\pi/(47d)$ S4.3

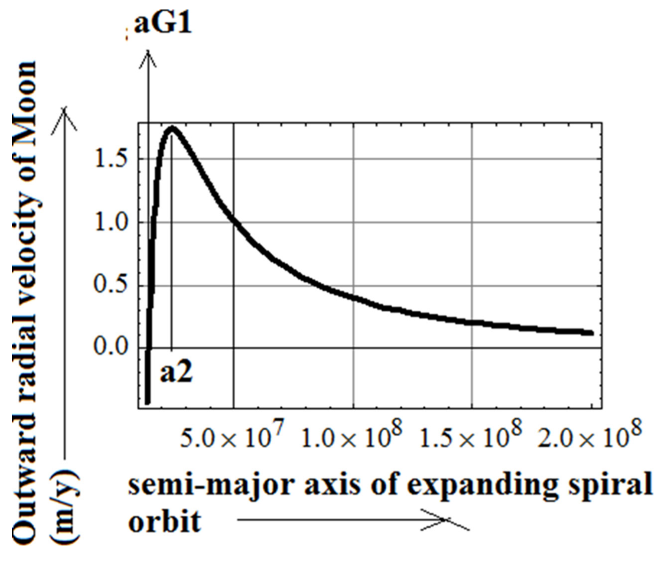

Figure S 4.1: Radial Velocity Profile of Moon from the birth to the final lock-in point at aG2. X-axis is semi-major axis. Y-axis is velocity in m/y.

Either it will remain stay put in this outer geo-synchronous orbit or it will be deflected back on an inward collapsing spiral orbit due to Sun's perturbation. Sir James Jeans [33] suggested that when our Moon will reach outer geo-synchronous orbit aG2 then Moon will be orbiting Earth in 47 days, Earth will be spinning in 47 days but its orbital period around Sun will be more than 365.25 d hence Earth will try to synchronize i.e. its spin will be try to equalize with orbital period hence Earth's spin period will further lengthen. As Earth's spin period becomes longer than 47 d, our Moon will fall in sub-synchronous orbit with respect to the Earth hence Moon will get trapped in a death spiral and eventually collapse into Earth. But much earlier Sun would have burnt all its fuel and become a Red Giant expanding to engulf Earth-Moon system [34]. Here a pertinent question arises. Why does Moon recede from Earth when it is trapped in gravitational potential well created by the Earth? Where does the energy come for climbing up the potential well? The answer is 'Gravitational

Sling Shot effect'.

4.1. What is Gravitational Sling Shot effect?

Planet fly-by, gravity assist is routinely used to boost the mission spacecrafts to explore the far reaches of our solar system [35-38]. Voyager I and II used the boost provided by Jupiter to reach Uranus and Neptune. Cassini has utilized 4 such gravity assists to reach Saturn. New Horizon space craft has used a similar Jupiter fly-by gravity assist in its interplanetary journey. By Jupiter flyby-gravity assist the journey to Pluto has been shortened by 3 years. In E-M system, planet fly-by gravity assist maneuver a space-craft which passes "behind" the moon gets an increase in its velocity (and orbital energy) relative to the primary body. In effect the primary body launches the space craft on an outward spiral path. If the spacecraft flies "infront" of a moon, the speed and the orbital energy decreases. Traveling "above" and "below" a moon alters the direction modifying only the orientation (and angular momentum magnitude). Intermediate flyby orientation change both energy and angular momentum. Accompanying these actions there are reciprocal reactions in the corresponding moon.

The above slingshot effect is in a three body problem. In a three body problem, the heaviest body is the primary body. With respect to the primary body the secondary system of two bodies are analyzed. In case of planet flyby, planet is the primary body and the moon- spacecraft constitute the secondary system.

While analyzing the planetary satellites, Sun is the primary body and planet-satellite is the secondary system. But in our analysis, Sun has been neglected. This results in errors leading to erroneous LOD formalism which has a poor match with observed LOD curve given in Table 1 of the main text. In fact the general trend of evolution of our Moon has been misanalysed in http://arXiv.org/abs/0805.0100 [39]

In my personal communication Laplace Plane transition and Cassini State Transition has not been taken into account.

Gravitational Sling Shot phenomena launched Moon on its Non-Keplerian Journey from (inner geo-synchronous orbit) aG1 to (outer geo-synchronous orbit) aG2. At inner and outer Geo-Synchronous Orbits, the Satellite is in Keplerian Orbit where centripetal and centrifugal forces are in equilibrium and radial acceleration and radial velocity are zero. But the Satellite is never allowed to stay in the inner Keplerian Orbits because it is energy maxima state as has been shown in subsequent section.

At the inner Geosynchronous Orbit slightest differential between ω and Ω and due to solar wind, cosmic particles or radiation pressure perturbation causes the Satellite to tumble out of the Keplerian Orbit. If the Satellite is long of aG1 it is launched on an outward expanding spiral path as our Moon is and if it is short of aG1 it is injected into an inward collapsing spiral path as Phobos (Martian Satellite) is launched. Initially at aG1 both Energy Conservation and Angular Momentum Conservation are maintained. Hence as soon as the Satellite tumbles out of the inner Geo-Synchronous Orbit it enters a Gravitational Runaway Phase. If it falls long of aG1, the Satellite experiences a powerful sling-shot effect because of rapid transfer of Planet's Spin Rotational energy to Satellite's Orbital energy. This causes an outward radial acceleration peaking at a1 as shown in Figure S4.2. The powerful sling-shot effect is like an impulsive torque.

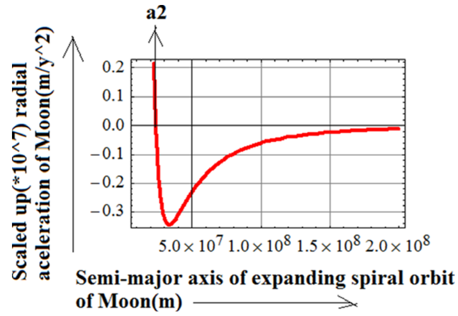

Figure S 4.2: Scaled up (× 10^7 times) Radial Acceleration Profile of Moon from birth to the final lock-in at aG2 X-axis is semi-major axis (m). Y-axis is acceleration in m/y2.

The sling-shot phase or Gravitational Runaway phase is damped out as the differential between ω and Ω grows and tidal dissipation increases. This leads to the termination of the Gravitational Runaway Phase at a2 where the Radial Acceleration becomes zero and Recession Velocity becomes maximum and where lom/lod=2. This point is also referred to as Gravitational Resonance point or 2:1 Mean Motion Resonance (MMR) orbit [40,41].

Thereafter the Satellite coasts along the outward spiral path on its own. Beyond a2, Radial acceleration is negative and Radial outward Velocity is continuously decelerated until it becomes zero at aG2.

In Figure S4.1 and Figure S4.2, the radial velocity profile and radial acceleration profile have been illustrated.

The profile is drawn from $1\times10^{\wedge}7m$ to $1\times10^{\wedge}8m$

At aG1=1.46 × 10^{7} m and at aG2=5.5335 × 10^{8} m, the radial velocity=0. These are the exact Keplerian equilibrium points. These are the triple synchrony orbits where the two components are tidally interlocked.

At a2 (2:1 Mean Motion Gravity Resonance orbit) where Radial Velocity is maximum and Radial acceleration is zero as shown in Figure S4.3.

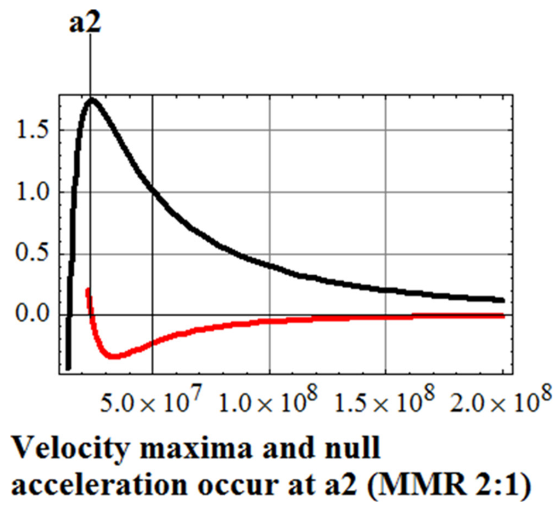

Figure S 4.3: Superposition of Radial Velocity Profile and Scaled up (× 10^7 times) Radial Acceleration Profile of Moon from birth to the final lock-in at aG2 . Note the coincidence of Radial Velocity maxima and null radial acceleration at a2 (MMR 2:1 orbital radius).

Short of aG1 the natural satellite is accelerated inward. Long of aG1 from aG1 to a2 (2:1 MMR gravity resonance orbit) the Moon is rapidly accelerated outward under the influence of an impulsive gravitational torque due to rapid transfer of spin rotational energy from Earth to Moon. The maxima of the outward radial acceleration occurs at A 1. (This is the peak of the impulsive sling shot torque).

From a1 to a2 the torque decays to zero because of the differential between ω and Ω leading to tidal dissipation. Hence up to a2 Moon is accelerated to a maximum velocity Vmax. Beyond a2, Moon climbs up the gravitational potential well and in the process gets decelerated. It reaches zero velocity at aG2. At this terminal point, it will remain stay put as Charon is stay put with respect to Pluto or it will spiral in because of third body perturbation. Moon will spiral-in because of Sun's perturbation [33].

S4.2. Deduction of outward radial velocity of Moon

In Kinematic Model, any binary system has two triple synchrony orbits which the Author refer to as inner and outer Clarke's Orbits and in Earth-Moon system they are referred to as inner geo-synchronous orbit (aG1) and outer geo-synchronous orbit (aG2).

Moon tidally evolves out of Inner Clarke's Orbit (aG1). If it tumbles short of aG1, secondary rapidly spirals-in to its certain destruction and if it tumbles long of aG1 then through Gravitational Sling Shot secondary is launched on an outward spiral path. But as the differential between orbital velocity and spin velocity of primary grows, tidal stretching and squeezing sets in the primary body which leads to tidal dissipation which causes a rapid exponential decay of the impulsive torque. In super synchronous orbit primary's tidal bulge leads the radius vector joining primary and secondary. This 'lead angle' causes secular deceleration of the primary and angular momentum transfer from primary to secondary for angular momentum conservation. From then onward the Moon coasts on its own until it locks into the outer Outer Clarke's Orbit (aG2). But throughout this tidal evolutionary history the

Total Angular Momentum is conserved hence we have the following Conservation of Momentum equation:

$$JT = C\omega + \left(m^* a_{present}^2 + I\right)\Omega = \left[C + \left(m^* a_{G1}^2 + I\right)\right]\Omega_{G1} = \left[C + \left(m^* a_{G2}^2 + I\right)\right]\Omega_{G2} \quad \text{... S4.4}$$

In (S4.4):

C=Moment of Inertia of the Primary around its spin axis. I=Moment of Inertia of the Secondary around its spin axis. And m*=reduced mass of the secondary=m/(1+m/M) where m=the mass of the secondary and M=mass of the primary.

From Kepler's Third Law:

$\Omega aG1 = B / aG1^\wedge(3/2)$ And $\Omega aG2 = B / aG2^\wedge 3/2$

Where $B = \sqrt{G(M+m)}$ ..... S4.5.

Substituting (S4.5.) in (S4.4.)

We get:

$$JT = C\omega + \left(m^* a_{present}^2 + I\right)\Omega = \left[C + \left(m^* a_{G1}^2 + I\right)\right] B / aG1^\wedge(3/2) = \left[C + \left(m^* a_{G2}^2 + I\right)\right] B / aG2^\wedge 3/2$$

$$JT = C\omega + \left(m^* a_{present}^2 + I + I\right)\Omega = \left[C + \left(m^* aG12 + I\right)\right] B\, aG13/2 = \left[C + \left(m^* aG22 + I\right)\right] B\, aG232$$

.... $S4.6$

Solving (S4.6), we get the two roots of the Binary System namely aG1 and aG2. In classical Newtonian Mechanics two triple synchrony orbits do exist from total energy consideration as shown in S5. Hence Author calls this model as Kinematic Model (KM). From Classical Mechanics the Synchronous Orbit is the same as the Inner Clarke's Orbit calculated in Kinematic Framework for vanishingly small mass ratio m/M. In Classical Mechanics, the synchronous orbit is defined as:

$$a_{sync}^{3/2}\,\Omega_{ORB} = a_{sync}^{3/2}\,\omega_{PRIMARY} = B \quad \text{... S4.7}$$

In Table S4.1, all cases are consistent with Kinematic Formalism except Pluto-Charon (case no.4). This exception is due to large uncertainty in the Globe-Orbit parameters of Pluto-Charon.

Table S4.1: Comparative Study of Triple Synchrony Orbits of Earth-Moon, Mars-Phobos Deimos, Pluto-Charon Systems, Sun-Jupiter and two stellar binaries (NN-Serpentis and RW Lac) from Classical Newtonian Mechanics and Kinematic Model. [The Globe-Orbit Parameters based on which the calculations have been made are given in S4 (Appendix A in supplementary materials).

Planet-Sat	Mass-ratio (q)	a (present) (m)	B ($m^{3/2}/s$)	a G1 (m)	a G2 (m)	async (m) from (S 4.7.)
Earth-Moon	1/81	3.84400×10^8	2.00811×10^7	1.46×10^7	5.53×10^8	4.234×10^7
Mars-Phobos	10^{-8}	9.378×10^6	6.54×10^6	2.04×10^7	7.46×101^8	2.04×10^7
Mars-Deimos	10^{-9}	23.459×10^6	6.54×10^6	2.04×10^7	1.69×10^{20}	2.04×10^7
Pluto-Charon	1/8	19.600×10^6	9.88×10^5	1.37672×10^6	1.95579×10^7	1.96133×10^7
Sun-Jupiter	9.55×10^{-4}	778.3×10^9	1.15256×10^{10}	1.06889×10^9	7.92465×10^{11}	2.53×10^{10}
NN-Serpentis	0.2074	6.49597×10^8	9.25989×10^9	4.44958×10^7	6.4986×10^8	6.49514×10^8
RW-Lac	0.9375	1.69267×10^{10}	1.54426×10^{10}	4.08908×10^8	1.69314×10^{10}	1.69252×10^{10}

Case 1: Moon is a significant fraction of Earth (1/81) hence our Moon has a definite Tidal Evolution History. It started its journey about 4.467 Gya (The birth of the Solar System is the time when the condensation of the first solid took place from the Solar Nebula. This is taken as 4.567 Gya. The last giant impact on Earth formed the Moon and initiated the final phase of core formation by melting the mantle of the Earth. The date of this last impact decides the birth date of Moon which was completed in a few hundred years by the accretion of the impact generated debris. Yin et.al [42], Jacobsen [43] and Taylor et.al [44] claim an age of Moon as 30 My after the birth of Solar System. Toubol et.al [45], Allègre, et.al [46] and Halliday and Wood claim an younger Moon formed after 50 to 100 My after the first solid condensed. The concentration of Highly Siderophile Elements (HSEs) in Earth's mantle constrains the mass of chondritic material added to Earth during Late Accretion [47,48]. Using HSE abundance measurements [49], Jacobson et.al [50] determine a Moon formation age of 95 ± 32 Myr after the condensation. This method is invariant of the geochemistry chronometer adopted by earlier researchers. So it will be realistic to take the age of Moon as 4.467 Gya. Since its birth just beyond Roche's Limit 15,000 Km. By gravitational sling shot it was launched on an expanding spiral orbit from inner geo-synchronous orbit of 15,000 Km orbital

radius towards the outer geo-synchronous orbit of 5.53×10^8 m=553,000 Km. At the inner geo-synchronous orbit, the length of day=length of month=5 hours and at the outer geosynchronous orbit, the length of day=length of month=47 days. Presently the lunar orbital radius is 384,400 Km with sidereal length of day=23.9344 hours and length of Sidereal Month=27.32 Earth days. Earth-Moon started from geo-synchrony and will end in geo-synchrony. As predicted in Figure 1, for mass ratio=1/81 the classical synchronous orbit is less than the outer geo-synchronous orbit.

Case 2 and 3: In case of Mars-Phobos-Deimos, since the mass ratio is insignificant hence Deimos launched on an orbit long of inner Clarke's Orbit has hardly evolved from its point of inception which is inner Clarke's Orbit. But Phobos is launched on an orbit short of inner Clarke's orbit hence it is on a gravitational runaway orbit, trapped in a death spiral. Deimos is stay-put in its orbit of inception which is 20,400 Km but Phobos has lost altitude from its point of inception of 20,400 Km to the present altitude of 9,378 Km. Since the mass ratio is insignificant hence the classical synchronous orbit is the same for both Phobos and Deimos equal to 20,400 Km same as the inner Clarke's Orbit. This is in exact correspondence with Figure 1.

Case 4: Pluto-Charon's classical synchronous orbit should be smaller than Outer Clarke's Orbit as required by Kinematic Analysis but the former is 0.28% larger. This is due to the uncertainty in Globe-Orbit parameters of Pluto-Charon.

Case 5: Mass ratio of Jupiter to Sun is 10^-3 hence according to KM analysis Jupiter-Sun has a tidal evolutionary history with a rapid Time-constant of evolution of 4.275 My. It has evolved from inner Clarke's Orbit 3.7859 × 10^9 m to the present orbit of 778.3 × 10^9 m where its evolution factor is 0.893 and eventually it will lock into second triple-synchrony state in the outer Clarke's Orbit of 871.161×10^9 m. The classical synchronous orbit is at 25.3 × 10^9 m, 97% smaller than outer Clarke's Orbit, as predicted by Figure S4.4 also.

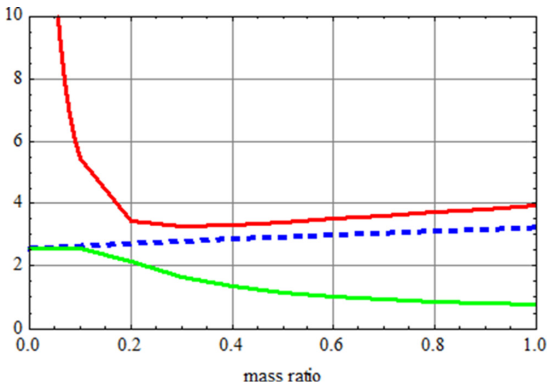

Figure S 4.4: Plot of asynSS (× RIap), aG1 (× RIap) and aG2 (× RIap) as a function of 'q'=mass ratio. Y-axis is semi-major axis as a multiple of Iapetus Globe Radius. **Note:** (--) asynSS, (–) aG1, (–) aG2

In Paper No. B0.3-0011-12 Iapetus hypothetical sub-satellite re-visited and it reveals celestial body formation process in the KM Framework. [resented at 39th COSPAR Scientific Assembly, Mysore, India from 14th July to 20th July 2012, the correspondence between Newtonian Formalism of Synchronous Orbit and Kinematic.

Case 6 and Case 7: These are stellar nonrelativistic binaries. I call them non-relativistic because the mean apisidal motion is negligible. Here since the mass ratio is greater than 0.2, hence the original molecular cloud settles into a binary in Months-Years and gets locked-into outer Clarke's Orbit. In both cases the synchronous orbit is shorter than the Outer Clarke's Orbit by 0.05% and 0.04% respectively. This is consistent with Kinematic Analysis.

Inspection of Figure S4.4, tells us that at infinitesimal values of 'q', asynSS is the same as aG1 and only one Clarke's Orbit is perceptible. But at larger mass ratios the two (classical and kinematic formalism for aG1) rapidly diverge. Author's analysis till now has confirmed that aG1 is the correct formalism for predicting the inner triple synchrony orbit in a binary system at q<0.2. At mass ratios greater than 0.2, aG1 is physically untenable and only aG2 is perceptible. Outer Triple Synchrony Orbit seems to converge but does not actually converge to the classical formalism but remains offsetted right till the limit of q =1. Here again only outer Clarke's Orbit is perceptible. The actual Star pairs satisfy the Kinematic formalism and not the classical formalism. So Kinematic Formalism, though satisfies the correspondence principle at q~0, is a theory in its own right. Till date there exists formalism for two triple synchrony orbits in Classical Newtonian Mechanics. In the mass ratio range 0.0001 to 0.2 through total energy analysis as shown in S5 the two triple synchrony orbis can be derived. For mass ratio less than 0.0001, binaries remain in inner Clarke's Configuration stably which is predicted by Classical Newtonian Formalism also. 61 At mass ratios greater than 0.2 right up to unity, star pairs remain in outer Clarke's Configuration stably and its magnitude is more than Newtonian prediction. For mass ratios 0.0001 <q < 0.2, Outer Clarkes configuration is the only stable orbit and secondary is catapulted from aG1 by Gravitational Sling Shot mechanism and it migrates out of that configuration. If it is at a > aG1 the pair spirals out with a time constant of evolution and if aAt mass ratios greater than 0.2 right up to unity, star pairs remain in outer Clarke's Configuration stably and its magnitude is more than Newtonian prediction.

For mass ratios 0.0001 <q <0.2, Outer Clarkes configuration is the only stable orbit and secondary is catapulted from aG1 by Gravitational Sling Shot mechanism and it migrates out of that configuration. If it is at a > aG1 the pair spirals out with a time constant of evolution and if a <aG1 then the pair spirals-in on a collision course again with a characteristic time constant of evolution.

Time Constant of Evolution is in inverse proportion of some power of mass ratio [15].

For q=0.0001, it is Gy and as q increases, time-constant decreases from Gy to My to kY to years. This is valid for mass scale encountered in Solar and Exo-Solar Systems. Between 0.2 to 1, a solar nebula falls into outer Clarke's Configuration by hydro-dynamic instability within months/years.

For q being vanishingly small, the calculation of the man-made Geo-synchronous Satellite's orbit of 36,000 Km above the equator has been done by Kinematic Formalism. This calculation has been done by the Author in his personal communication: http://arXiv.org/abs/0805.0100.

S4.2.1. Deductions of the kinematic parameter of E-M system: Using Globe-Spin parameters of E-M system given in Appendix A of S4, we get the following kinematic parameters:

Reduced mass of Moon=m/(1+m/M)=m*=7.25284 × 10^{22} Kg

B=√(G(M+m))=2.00811 × 10^7 m^3/2/s, G=6.67 × 10^{-11} m3/(kg-s2),

C=moment of inertia of Earth around its spin axis=0.33086 MR2=8.0209 × 10^{37} Kg-m2,

I=moment of inertia of Moon around its spin axis=0.394 mRmoon2=8.72791 × 10^{34} Kg-m2,

Define θ1=I/C =0.00108815, θ2=m*/C=9.04243 × 10^-16 1/m2,

JT=Total angular momentum of E-M system=3.43584 × 10^{34} Kg-m2/s,

Spin Period of Earth=1 Solar Day =24 hours.

Sidereal Spin Period of Moon=27.322 Solar Day,

Sidereal Orbital period of E-M system=27.3217 Solar Day,

Moon is in synchronous orbit i.e. it is tidally locked and shows the same face to Earth. Generally this synchronism property is true for all compact binaries. Because of this synchrony 62 of our Moon and because of the circular path, our Moon experiences no stretching and squeezing and hence no tidal heating and hence no volcanic effect. 'Io', a moon of Jupiter, is similarly placed as our Moon is with respect to Earth but still Io is the most volcanically active natural satellite because of tidal dissipation. In synchronous orbit there should have been no volcanic activity but its eccentric orbit makes it the most volcanically active natural satellite in our solar system. Io is in 2:1 resonance with Europa hence it has eccentric orbit and hence it is evolving and gradually circularizing. As its eccentricity is reduced in the process of circularization, the volcanic activity is on the wane.

Solving (S3.6) we obtain the two geo-synchronous orbits:

$aG1 = 1.46402\times10^{\wedge}7m$, $aG2 = 5.5247\times10^{\wedge}8S4.8$ ... S4.8

According to Ida and Stewart [12], tidal flexing does not allow the solid particles to coalesce within Roche's limit represented by the symbol aR.

$aR = 2.456(\rho E\rho M)^{\wedge}1/3RE \sim 2.9RE = 18496.606\,Km$ ... S4.9

Where $\rho E = 5.5gm/cc$ and $\rho M = 3.34gm/cc$ ... S4.9

And Roche Zone is defined within the range: 0.8 to 1.35 aR or 2.32 to 3.915 R_E i.e. within 14,797 km to 24,970 km

This implies that impact generated debris will be prevented from accretion within 1.48 × 10^7 m and those in 1.48 × 10^7 m to 2.5 × 10^7 m range also known as transitional zone will experience limited accretion growth whereas those lying beyond this zone will be unaffected by tidal forces. It is a happy coincidence that the Roche zone lies just beyond the inner Geo-Synchronous orbit of the Earth-Moon System. This implies that if accretional criteria of Canup and Esposito [51] is satisfied along with the impact velocity condition that is the rebound velocity should be smaller than the mutual surface escape velocity then merged body formation of Moon starts within the Roche zone. The accreted Moon gradually migrates outward sweeping the remnant debris.

S4.2.2. Deduction of LOM/LOD or ω/Ω equation:

Rewriting (S4.6) we obtain:

$$\frac{J_T}{C\Omega} = \left[\frac{\omega}{\Omega} + \left(\left(\frac{m^*}{C}\right)a^2_{present} + \frac{I}{C}\right)\right] = \left[\frac{\omega}{\Omega} + \theta_2 a^2_{present} + \theta_1\right] \text{....S4.10}$$

Substituting: $\Omega = B/a3/2$ in (S4.10) we obtain: 63

$$\frac{J_T}{CB}a^{3/2} = \left[\frac{\omega}{\Omega} + \theta_2 a^2_{present} + \theta_1\right] \text{.... S4.11}$$

Rearranging the terms in (S4.11) we get:

$$\frac{\omega}{\Omega} = \frac{LOM}{LOD} = \frac{J_T}{CB}a^{3/2} - \left(\theta_2 a^2 + \theta_1\right) = Aa^{3/2} - Fa^2 \text{.. S4.12}$$

where $A = \frac{J_T}{CB}$ and $F = \left(\theta_2 + \frac{\theta_1}{a^2}\right)$ S.12

Substituting the numerica values we get: Substituting the numerical values of the parameters we get:

$A = 2.1331\times10-11(1/m3/2)$ and $F = 9.0425\times10-16(1/m2)$

Substituting these values in (S4.10) we get LOM/LOD =27.1479.

The actual value of LOM/LOD is 27.322. This error is due to uncertainty in Globe-Spin parameters. A and F are adjusted to obtain the exact value of 27.322.

The best fit values of LOM/LOD constants are:

$A = 2.13853\times10-11(1/m3/2)$ and $F = 9.05842\times10-16(1/m2)$

The best fit parameters give the following geo-synchronous orbits:

ag1=1.46402 × 10^7 m, ag2=5.5247 × 10^8, a2=2.40649 × 10^7 m ... S4.13

Calculating LOM/LOD in (S4.12) using the best fit parameters of 'A' and 'F' we get:

LOM/LOD=27.322 which is the present era Sidereal Lunar Month/Solar Day observed values.

S4.2.3. The Tidal Torque formalism and Radial Velocity formalism: For the calculation of the spiral trajectory we need the radial velocity of recession in case of super-synchronous configuration and velocity of approach in case of sub-synchronous configuration. The time integration of the reciprocal of radial velocity gives the non-Keplerian Transit time from its inception to the present orbit. This transit time should be equal to the age of the secondary or the natural satellites. The starting point of this time integral will be the tidal torque.

The Tidal Torque of Satellite on the Planet and of Planet on the Satellite=Rate of change of angular momentum hence $TidalTorque = T = dJorb/dt$ ...S4.14

But Orbital Angular Momentum: 64

$$J_{orb} = m^* a^2 \times \frac{B}{a^{3/2}} = m^* B\sqrt{a} \text{..... S4.15}$$

Time Derivative of (S4.15) is: $T = \frac{dJ_{orb}}{dt} = \frac{m^* B}{2\sqrt{a}} \times \frac{da}{dt}$ S4.16

In super-synchronous orbit, the radius vector joining the satellite and the center of the planet is lagging planetary equatorial tidal bulge hence the satellite is retarding the planetary spin and the tidal torque is BRAKING TORQUE.

In sub-synchronous orbit, the radius vector joining the satellite and the center of the planet is leading planetary equatorial tidal bulge hence the satellite is spinning up the planet and the tidal torque is ACCELERATING TORQUE.

These two kinds of Torques are illustrated in Figure S3.1 and Figure S3.2.

I have assumed the empirical form of the Tidal Torque as follows:

$$T = \frac{K}{a^Q}\left[\frac{\omega}{\Omega} - 1\right] \text{.... S4.17}$$

(S4.17) implies that at Inner Clarke's Orbit and at Outer Clarke's Orbit, tidal torque is zero and (S4.16) implies that radial velocity at Inner Clarke's Orbit and at Outer Clarke's Orbit, is zero and there is no spiral-in or spiral-out.

At Triple Synchrony, Satellite-Planet Radius Vector is aligned with planetary tidal bulge and the system is in equilibrium. But there are two roots of ω/Ω=1: Inner Clarke's Orbit and Outer Clarke's Orbit. It has been shown in S5 that in Total Energy Profile, Inner Clarke's Orbit aG1 is energy maxima and hence unstable equilibrium state and Outer Clarke's Orbit aG2 is energy minima and hence stable equilibrium state. In any Binary System, secondary is conceived at aG1. This is the $CONJECTUR_E$ assumed in Kinematic Model. From this point of inception Secondary may either tumble short of aG1 or tumble long of aG1. If it tumbles short, satellite gets trapped in Death Spiral and it is doomed to its destruction. If it tumbles long, satellite gets launched on an expanding spiral orbit due to gravitational sling shot impulsive torque which quickly decays due to the growing differential of ω/Ω and the resulting tidal heating. After the impulsive torque has decayed, the satellite coasts on it own toward final lock-in at aG2.

Equating the magnitudes of the torque in (S4.16) and (S4.17) we get:

$$\frac{m*B}{2\sqrt{a}} \times \frac{da}{dt} = \frac{K}{a^Q}\left[\frac{\omega}{\Omega} - 1\right] \text{.. S4.18}$$

Rearranging the terms in (S4.18) we get: 65

$$V(\mathrm{a}) = \frac{da}{dt} = Velocityofrecession = \frac{2K}{m*B} \times \frac{1}{a^Q}[Aa^2 - Fa^{2.5} - \sqrt{a}]\mathrm{m/s} \text{ ..... S4.19}$$

The Velocity in (S4.19) is given in m/s but we want to work in m/y therefore (S4.19) R.H.S is multiplied by 31.5569088 × 10^6 s/(solar year).

$$V(\mathrm{a}) = \frac{2K}{m*B} \times \frac{1}{a^Q}[Aa^2 - Fa^{2.5} - \sqrt{a}] \times 31.5569088 \times 10^6]\frac{m}{y} \text{ ...... S4.20}$$

In (S4.20) 'a' refers to the semi-major axis of the evolving Satellite. There are two unknowns: exponent 'Q' and structure constant 'K'. Therefore two unequivocal boundary conditions are required for the complete determination of the Velocity of Recession.

First boundary condition is at a=a2 which is a Gravitational Resonance Point where ω/Ω=2 [38],

i.e. (Aa^3/2–Fa^2)=2 has a root at a2.

In E-M case, a2=2.40649 × 10^7 m.

At a2 the velocity of recession maxima occurs. i.e. V (a2)=Vmax.

Therefore at a=a2, (δV(a)/δa)(δa/δt)|a2=0.

On carrying out the partial derivative of V (a) with respect to 'a' we get the following: At a2, (2−Q) × a^1.5−(2.5−Q)F × a2−(0.5−Q)=0 ...... S4.21

Solving (S3.21) at 2:1 Mean Motion Resonance orbit 'a2' we obtain: Q=3.23771 ....S4.22

Now structure constant (K) has to be determined. This will be done by trial error so as to get the right age of Moon (Foot note 5) i.e. 4.467 Gy. Rewriting (S4.20) and substituting the best fit values of the exponent and constants A and F we obtain the structure constant 'K'.

$$V(\mathrm{a}) = \frac{2K}{m*B} \times \frac{1}{a^Q}[Aa^2 - Fa^{2.5} - \sqrt{a} \times 31.5569088 \times 10 \text{ ..... S3.23}$$

We will assume the age of Moon 4.46 Gy as already mentioned in Case 1 of subsection 4.2. The Transit Time from aG1 to the present 'a' is given as follows:

$$Transit\,Time = \int_{aG1}^{a} \frac{1}{V(a)}da \text{ ... S4.24}$$

Assuming a tentative value for Vmax and inserting it in (S3.23) at a=a2 we deduce the value of 'K'. Using this 'K' in (S3.23) and inserting this trial expression in (S3.24) we carry out the time integral to get the transit time from aG1 to present 'a' which should be the age of Moon as agreed upon 4.467 Gy. Several iterations are carried by adjusting Vmax. By this iteration method we obtain the best fit structure constant as:

$$K = 6.48548 \times 10^\wedge 42\left(Newton - m^\wedge(Q+1)\right) \text{ ... S4.25}$$

So the best fit velocity of recession formalism is:

$$V(a) = 2 \times 6.48548 \times 10^\wedge 42/(m*B) \times 1/a^\wedge 3.23771\left[A \times a^\wedge 2 - F \times a^\wedge 2.5 - \sqrt{a}\right] \times 31.5569088 \times 10^\wedge 6m/y$$

... S4.26

Transit Time expression gives 4.4635 Gy using (S4.24). This is the age of Moon as concluded previously.

Present recession velocity of Moon =2.3244 cm/y ... S4.27

LLR measurement of Moon's recession is anomalously higher than the calculated value.

This is the first indication that KM is oversimplified and not giving the correct result. The velocity of recession of Moon, the deceleration of Moon and the superposition of the two are shown in Figure S3.1, Figure S3.2.

S4.3. The theoretical formalism of lengthening of day curve poorly validated by observed LOD curve

Paleontologists have studied the length of day in the past geological epochs. John West Wells [6,7] through the study of daily and annual bands of Coral fossils and other marine creatures in bygone era has obtained ten benchmark. Leschiuta andTavella [52] and Kaula and Harris [8] have given the estimate of the synodic month based on the study of marine creature fossils. From the synodic month we can estimate the length of the Solar Day as given in S4. Appendix [B]. But the estimate in of LOD by synodic month is always an over-estimation hence the estimated LOD from synodic month have been rejected. In S4 Appendix [B] the estimation of LOD from synodic method and their over-estimation has been tabulated. One benchmark has been provided by Charles P Sonnett et al [9], through the study of tidaliesin ancient canals and estuaries. He gives an estimate of LOD=18.9 h at about 900 million years B.P. in Proterozoic Eon, pre-Cambrian Age. Arbab [53] has estimated LOD from the data of John West Wells and from cosmological consideration hence including Arbab data we have all together 24 data set which have been tabulated in Table S4.1. Using (S3.26) the orbital radius corresponding to the geologic epoch of observation has been calculated and tabulated in Column 3 of Table S4.1. From Table S4.2, the observed lengthening of day curve is generated as shown in Figure S4.5.

Table S4.2: Observed Length of Day in different geological epochs as calculated in KM.

Data set #	Time B.P. (years)	Orbital radii (m)†	LOD (hrs)[1]	LOD[2] (hrs)
1	Present	3.844×10^8	24	24
2	65 Ma	3.8287×10^8	23.627	23.6
3	135 Ma	3.81213×10^8	23.25	NA
4	136 Ma	3.8118×10^8	23.2515	23.2
5	180 Ma	3.80129×10^8	23.0074	23
6	230 Ma	3.7891×10^8	22.7683	22.7
7	280 Ma	3.7768×10^8	22.4764	22.4
	300 Ma	3.7718×10^8	22.3*	
8	345 Ma	3.76055×10^8	22.136	22.1
9	380 Ma	3.7517×10^8	21.9	NA
10	405 Ma	3.74535×10^8	21.8055	21.7
11	500 Ma	3.7208×10^8	21.276	21.3
12	600 Ma	3.6943×10^8	20.674	20.7
13	715 Ma	3.663×10^8	NA	20.1
14	850 Ma	3.6251×10^8	NA	19.5
15	900 Ma	3.61075×10^8	18.9	19.2
16	1200 Ma	3.5205×10^8	NA	17.7
17	2000 Ma	3.235×10^8	NA	14.2
18	2500 Ma	3.012×10^8	NA	12.3
19	3000 Ma	2.735×10^8	NA	10.5
20	3560 Ma	2.3143×10^8	NA	8.7
21	4500 Ma	NA	NA	6.1

Note: [1]Length of Day according to John West Wells [6,7], and Charles P Sonnet [9]; [2]Length of Day according to Arbab [53]; *Length of Day according to Leschiutta and Tavella [52]; †Orbital Radius of Moon calculated from KM for classical Moon.

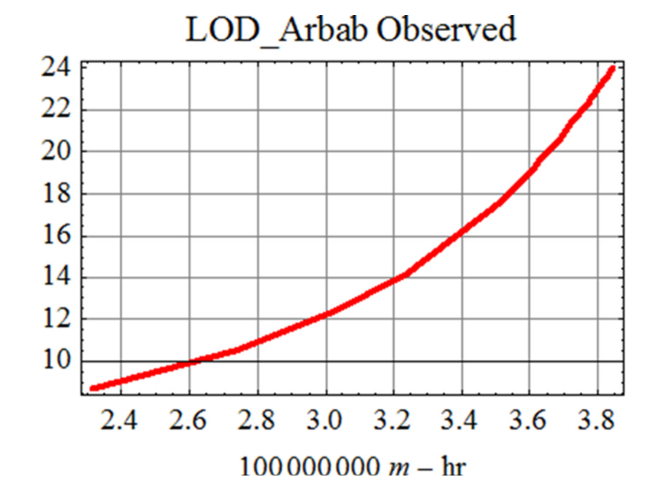

Figure S 4.5: Observed Lengthening of Day curve over a time span of 3.56 Gy.

S4.3.1.Theoretical formalism of length of earth day in the entire life span of Moon: From Kepler's Third Law:

$$T_{orb} = \frac{2\pi\times a^{3/2}}{B} \quad \text{... S3.28}$$

$$\frac{\omega}{\Omega} = \frac{LOM}{LOD} = \frac{J_T}{CB} a^{3/2} - \left(\theta_2 a^2 + \theta_1\right) = Aa^{3/2} - Fa^2 \quad \text{....S4.12}$$

$$\frac{T_{orb}}{T_E} = (Aa^{3/2} - Fa^2) \quad \text{....S4.29}$$

Substituting (S3.28) in (S3.29) we obtain LOD:

$$T_E = \frac{2\pi\times a^{3/2}}{B(A\times a^2 - F\times a^2)} \quad \text{....S4.30}$$

Substituting the best fit parameters in (S4.30) the theoretical lengthening of day curve is obtained in Figure S4.6.

Superposition of the theoretical curve and observed curve gives Figure S4.7.

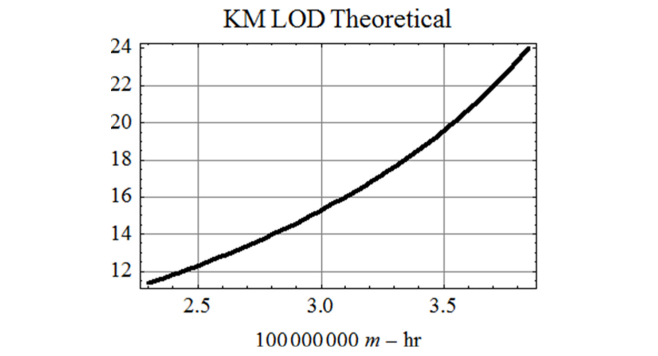

Figure S 4.6: Theoretical Lengthening of Day curve over a time span of 3.56 Gy

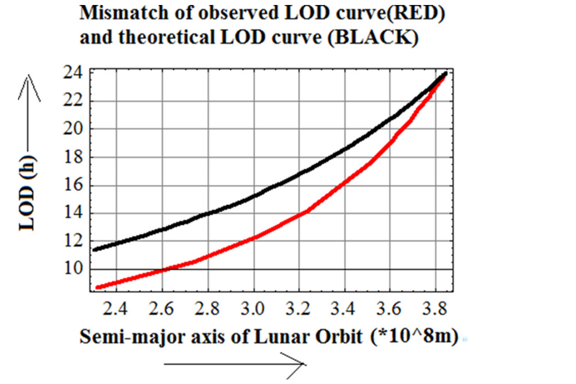

Figure S 4.7: Superposition of Theoretical and Observed Lengthening of Day curve over a time span of 3.56 Gy. The worst case mismatch is 31%.

Clearly there is a mismatch over the entire time span with the worst case scenario occurring at 3.56 Gy ago. The worst case mismatch is -31%.

Needless to say KM has failed to capture the true picture of tidally coupled Earth-Moon.

S5. APPENDIX (A) AND APPENDIX (B) OF S3 AND S4

Appendix (A).Globe-Spin parameters of Earth-Moon system

http://nssdc.gsfc.nasa.gov/planetary/factsheet/moonfact.html as shown in Figure S6.1.

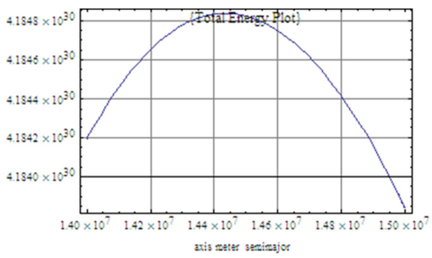

Total Energy Plot from a=1.4*10^7m to a=1.5*10^7m

Inner Geosynchronous Orbit= aG1=1.46177*10^7m

Figure S 6.1: Plot of total energy in the range 1.4 × 10^7 m and 1.5 × 10^7 m around the inner geo-synchronous orbit of a=1.46 × 10^7 m.

Appendix (B) Determination of LOD from the synodic month in a given geologic epoch

Leschitua and Tavella [52] and Kaula and Harris [8] have estimated the synodic month in the past epochs. Their measurements are given in Table S5 B1.

Table S5. B1: Estimation of LOD from synodic month and from paleobotanical and paleotidal evidences.

T(B.P.)	T*	Synodic Month	Orbital radius	Estimated LOD	LOD by Wells
900 Ma	3.56347 Gy	25 d	3.61075×10^8 m	19.8362 h	18.9 h
600 Ma	3.86347 Gy	26.2 d	3.6943×10^8 m	20.9669 h	20.674 h
300 Ma	4.16347 Gy	28.7 d	3.7718×10^8 m	23.0519 h	22.3 h
45 Ma	4.41847 Gy	29.1 d	3.8335×10^8 m	23.6 h	NA
2.8 Ga	1.66347 Gy	17 d	2.8537×10^8 m	13.5569 h	NA

The methodology of determination of LOD from Synodic Month

$$T_{synodic} = \frac{T_{sidereal}}{1-\frac{T_{sidereal}}{Z}} = \frac{\frac{LOM}{LOD}\times T_E d}{1-\frac{\frac{LOM}{LOD}\times T_E d}{Z}}$$

where $T_{sidereal}$ =actual orbital period and

$$Z = \frac{365.242d/y}{T_E(d)} \text{ =where } T_E = Earth\,day \quad ......S5.B1$$

From the geologic epoch the corresponding orbital radius is determined. Using the orbital radius of the given geologic epoch and (S4.28), LOM/LOD is determined.

Using S5.B1 we get the Earth day corresponding to a synodic month and tabulated in Table S5B.2.

Table S5. B2: Comparative study of LOD from synodic method and those obtained from coral fossils and tidalites

Geologic epoch	a (orbital radii)	LOM/LOD	Synodic month	LOD1	LOD2
900 Ma	3.61075×10^8 m	28.6282	25 d	19.8362 h	18.9 h
600 Ma	3.6943×10^8 m	28.2216	26.2 d	20.9669 h	20.674 h
300 Ma	3.7718×10^8 m	27.7835	28.7 d	23.0519 h	22.3 h
45 Ma	3.8335×10^8 m	27.3924	29.1 d	23.6 h	NA
2.8 Ga	2.8537×10^8 m	29.3245	17 d	13.5569 h	NA

Note: LOD1 is the estimate from Synodic month; LOD2 is the estimate from corals and tidalites. Clearly LOD obtained from synodic month are highly over estimated and hence rejected in this study.

S5.1. Kinematic Model yields two geo-synchronous orbits of E-M system validated by total energy analysis

The total energy analysis is utilized in case of E-M and the extremum points are obtained. The energy maxima happens to be the inner unstable geo-synchronous orbit (aG1) and the energy minima happens to be outer stable geo-synchronous orbit(aG2) in case of E-M and M-P systems and their values from KM correspond to those obtained from Energy Analysis. This vindicates KM of binary pairs.

S5.1.1. To determine the energy extremum points from total energy profile of E-M binary system: Total Energy of Earth-Moon System=Rotational Kinetic Energy+Potential Energy+Translational Kinetic Energy.

Translational Kinetic Energy of the order of 1×10^8 Joules due to recession of Moon for all

Practical purposes is negligible as compared to Rotational Kinetic Energy of the order of 1 × 10^30 Joules. Hence Translational Kinetic Energy is neglected in future analysis.

Moon is trapped in potential well created by the Earth.

Moon's potential energy=$-GM_{Earth}M_{Moon}/a$

G=Gravitational Constant=6.673×10^{-11} N-m2/Kg2;

M_{Earth}=mass of the Earth =5.9742×10^{24} Kg;

M_{Moon}=mass of the Moon =E/81 =7.348×10^{22} Kg;

a=semi-major axis of Moon's orbit around the Earth=3.844×10^8 m;

Rotational Kinetic Energy of Earth-Moon System=Spin Energy of the Earth+Orbital Energy of the Earth-Moon System+Spin Energy of the Moon=

$$\frac{1}{2}C\omega^2 + \frac{1}{2}\left(\frac{M_{Moon}}{1+\frac{M_{Moon}}{M_{Earth}}}\right)\times a^2 \times \Omega^2 + \frac{1}{2}(0.4M_{Moon}R^2_{Moon})\Omega^2 \quad .... S5.2$$

Where C=moment of inertia of Earth around polar axis =

0.3308 $M_{Earth}R_{Earth}$2=8.02×10^{37} Kg-m2; Equatorial Radius of Earth=6.37814×10^6 m;

Equatorial Radius of Moon=1.738×10^6 m;

Earth angular spin velocity=ω=2π/TE=[2π /(86400)] radians/sec;

In this analysis we will consider all rates of rotation to be in Solar Days. We will consider one solar day as the present spin-period of Earth. Similarly while calculating Earth-Moon orbital angular momentum we will use present sidereal month expressed in 27.3 solar days.

Earth-Moon Orbital Angular Velocity=Ω=[2π/(27.3 × 86400)] radians/sec where sidereal month =27.3 d;

Since Moon is in synchronous orbit i.e. it is tidally locked with the Earth hence we see the same face of Moon and Moon's Orbital Angular Velocity=Moon's Spin Angular Velocity=Ω;

$$KE=\frac{1}{2}C\omega^2+\frac{1}{2}\left(\frac{M_{Moon}}{1+\frac{M_{Moon}}{M_{Earth}}}\right)\times a^2\times\Omega^2+\frac{1}{2}(0.4M_{Moon}R^2_{Moon})\Omega^2 \quad \text{... S5.2}$$

Reshuffling the angular velocity terms we get:

$$KE=\frac{1}{2}\Omega^2[C\left(\frac{\omega}{\Omega}\right)^2+\left(\frac{M_{Moon}}{1+\frac{M_{Moon}}{M_{Earth}}}\right)\times a^2+(0.4M_{Moon}R^2_{Moon})] \quad \text{.....S5.3}$$

Substituting S4.12 in S5.33 we get:

$$KE=\frac{1}{2}\Omega^2[C\left(\mathrm{A}a^{3/2}-\mathrm{F}a^2\right)^2+\left(\frac{M_{Moon}}{1+\frac{M_{Moon}}{M_{Earth}}}\right)\times a^2+(0.4M_{Moon}R^2_{Moon}) \quad \text{.....S5.4}$$

According to Kepler's 3rd Law:

$$a^3\Omega^2=G\left(M_{Earth}+M_{Moon}\right)$$

Substituting S5.5 in S5.4 we get

$$KE=\frac{1}{2}\times\frac{G\left(M_{Earth}+M_{Moon}\right)}{a^3}[\left[\mathrm{C}\left(\mathrm{A}a^{3/2}-\mathrm{F}a^2\right)^2+\left(\frac{M_{Moon}}{1+\frac{M_{Moon}}{M_{Earth}}}\right)\times a^2+\left(0.4M_{Moon}R^2_{Moon}\right)\right] \text{.S5.36}$$

Therefore total energy=KE+PE

Thererfore

$$TotalEnergy=\frac{1}{2}\times\frac{G\left(M_{Earth}+M_{Moon}\right)}{a^3}[[\mathrm{C}\left(\mathrm{A}a^{3/2}-\mathrm{F}a^2\right)^2+\left(\frac{M_{Moon}}{1+\frac{M_{Moon}}{M_{Earth}}}\right)\times a^2+\left(0.4M_{Moon}R^2_{Moon}\right)]-\frac{G\left(M_{Earth}+M_{Moon}\right)}{a}$$

....S5.7

To determine the stable and unstable equilibrium points in non-Keplerian journey of Moon we must examine the Plot of Equation S5.7 from 'a' =8 × 10^6 m to 'a' =6 × 10^8 m Figure S6.1.

Table S5.1: Fact Sheet of Earth-Moon.

Parameters	Earth	Moon
Mass (Kg)	5.9726 × 10^{24}	0.07342 × 10^{24}
GM (Km3/s2)	0.3986 × 10^6	0.0049 × 10^6
Volumetric Mean Radius	6371	1737
Or Median Radius (× 10^3 m)		
Flattening (ellipticity)	0.00335	0.0012
Mean Density (Kg/m^3)	5514	3344
Moment of Inertia (I/(MR2))	0.33086	0.394
Sidereal Spin period	23.9344h	27.322d
Sidereal Orbital period (d)	-	655.7208 h (27.3217 d)
a* (semi-major axis) (× 10^8m)	-	3.84400
Lunar Orbit eccentricity	-	0.0549
Lunar Orbital Inclination with respect to Ecliptic	-	5.145 degrees
B=√(G(M+m))(m^3/2/s)		2.00873 × 10^7

Note: *Mean Orbital Distance from the center of Earth

We find an energy Maxima at inner geo-synchronous orbit (aG1=1.46 × 10^7 m) hence it is unstable equilibrium point. When Moon is at inner-geosynchronous orbit, any perturbation launches Moon on either a sub-synchronous orbit or on extra-synchronous (or super-synchronous orbit). If it is launched on sub-synchronous orbit then it rapidly spirals in towards the primary body and if it is launched on extra-synchronous orbit then it spirals out from inner to outer geo synchronous orbit. In our case, Moon is fully formed beyond Roches' Limit which is 18,000 Km just beyond inner Geo-synchronous Orbit hence Moon is launched on expanding spiral orbit towards outer Clarke's Orbit or outer Geo-synchronous Orbit [13].

As seen in Figure S5.2 at outer geosynchronous orbit (aG2=5.527 × 10^8 m.) there is energy minima hence it is stable equilibrium point. Secondary body can never move beyond this orbit.

Either it is stay-put in that orbit or it gets deflected back into a contracting spiral orbit.

The outer Geosynchronous Orbit defines the sphere of gravitational influence of Earth in much the same way as Hill Radius does for Earth in presence of Sun.

$$HillRadius=R_H=R\times\left(\frac{M_{+}}{M_{\circ}}\right)^{1/3} \quad \text{.....S5.8}$$

R =1AU=1.49598 × 10^{11} m.

Substituting the mass of Earth and Sun, Hill Radius is 1.49 × 10^9 m whereas aG2=5.527 × 10^8 m.

The results of KM are validated by an alternate method namely total energy profile analysis method

S6. THEORETICAL FORMALISM OF OBSERVED LOD WITHIN AKM FRAMEWORK

(The methodology of LOD theoretical formalism is given in Protocol Exchange URLhttp://doi.org/10.1038/protex.2019.017

S6.1.Data set of observed LODs known with high confidence level

John West Wells [6,7] using coral fossils and geo-chronometry has given 10 data points: Length Of Day (LOD)in hours extending from the present time to pre-Cambrian era.

Kaula and Harris [8] have given two data points. Charles P. Sonnet and Chan [9] have given one data point at 900 Ma. Leschiuta and Tavella [52] have given 3 data point. Arbab [53] has given 18 data points.

For analysis purposes Leschiuta and Tavella [52] and Kaula and Harris [8] dataset have been rejected because LOD in those cases are based on synodic months and synodic months give an over-estimation of LOD as shown in S4 Appendix B.

LODs dataset known with high level of confidence have been tabulated in Table S6.1

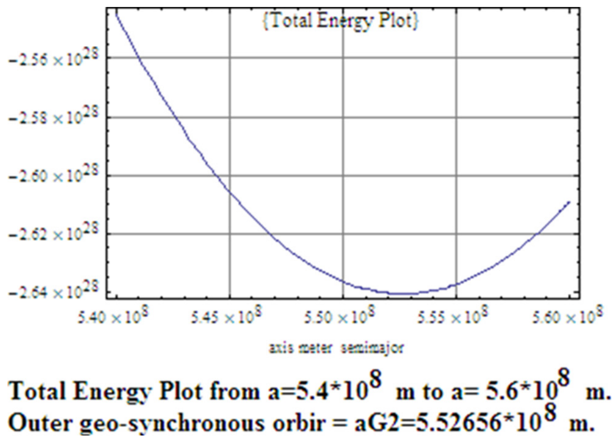

Figure S 5.2: Plot of total energy in the range 5.4×10^8 m and 5.6×10^8 m around the outer geo- synchronous orbit of aG2=5.527×10^8 m.

Table S6.1: List of LODs and their corresponding geological epochs.

Dat a set#	Time B.P.(years)[1]	Orbital radii (× 10^8 m)[2]	Orbital radii (× 10^8 m)[3]	V(a)[4] (cm/y)	LOD(h)	Comme nt
1	Present	3.844=60.336 R_E	3.844=60.336 R_E	3.7	24	
	45 Ma		3.8275=60.07 R_E		23.566 [1]	[8]
2	65 Ma	3.8287=59.63566 R_E	3.8198=59.965 R_E	3.755	23.627 [6,7]	[6,7]
3	135 Ma	3.81213=59.83566 R_E	3.79315=59.547 R_E	3.814	23.25 [6,7]	[6,7]
4	136 Ma	3.8118=59.83 R_E	3.7927=59.54R_E	3.815	23.2 [53]	[53]
5	180 Ma	3.80129=59.6655 R_E	3.7756=59.27R_E	3.8526	23 [6,7]	[6,7]
6	230 Ma	3.7891=59.474 R_E	3.7558=58,96R_E	3.897	22.7684 [6,7]	[6,7]
7	280 Ma	3.7768=59.28 R_E	3.7357=58.645 R_E	3.94	22.4765 [6,7]	[6,7]
	300 Ma		3.7275=58.516 R_E		22.3 [52]	[52]
8	345 Ma	3.76055=59.28 R_E	3.7068=58,19R_E	4	22.136 [6,7])	[6,7]
9	380 Ma	3.7517=58.887 R_E	3.69418=57.99 R_E	4.034	21.9 [6,7]	[6,7]
10	405 Ma	3.74535=58.787 R_E	3.6825=57.8257 R_E	4.05815	21.8 [6,7]	[6,7]
11	500 Ma	3.7208=58.4 R_E	3.6422=57.177 R_E	4.15	21.27 [6,7]	[6,7]
12	600 Ma	3.6943=57.986 R_E	3.5968=56.4646 R_E	4.25357	20.674, 20.7 [6,7,52]	[6,7,52]
13	715 Ma	3.663=57.495R_E	3.5423=55.609 R_E	4.377	20.1 [53]	[53]
14	850 Ma	3.6251=56.9 R_E	3.4748=54.549 R_E	4.531	19.5 [53]	[53]
15	900 Ma	3.61075=56.67 R_E	3.4485=54.1365 R_E	4.59	18.9, 19.2 [9,52,53]	[9,52,53]
16	1200 Ma	3.5205=55.26 R_E	3.2775=51.452 R_E	4.98	17.7 [53]	[53]
17	2000 Ma	3.235=50.8 R_E	2.6=40.8 R_E (not permissible)†	Oscillator yIn AKM	14.2 [53]	[53]
	2450 Ma (3.28 × 10^8m)		1.96=30.7 R_E (not Permissible)†	Oscillator yIn AKM		
18	2500 Ma	3.012=47 R_E			12.3 [53]	[53]
19	3000 Ma	2.735=43 R_E				
20	3560 Ma	2.3143				
21	4500 Ma	0.18				

Note: [1]Based on annual bands in coral fossils; [2]Orbital radii based on monotonically evolving Moon with Moon's age 4.467 Gy (KM); [3]Orbital radii based on accelerated Moon. (AKM); [4]Velocityofrecession of Moon based on presently accelerated Moon (AKM); †33 R_E orbital radius is Cassini State Transition orbit where E-M system become sun stable due to the transition in Lunar Spin axis from State1 to State2

33 R_E orbital radius is Cassini State Transition orbit where E-M system becomes unstable due to the transition in Lunar Spin axis from State1 to State2.

Table S6.1 clearly brings out the analogy of our classical Moon and the real Moon with tortoise and hare parable. Our classical Moon was slow and steady but our real Moon first moved in fits and interruptions and in the last 1.2 Gy real Moon has bounded to its goal. Real Moon has raced to its present orbit and hence we see 3.82 ± 0.07 cm/y lunar orbital recession rate which is anomalously high recession rate indicative of anomalously high tidal dissipation rate in Earth.

Advanced Kinematic Model of Earth-Moon system was introduced in CELE-D-17-00144 and is described in Sharma [52]. It is being us adhere to predict the theoretical LOD curve.

Earth's obliquity angle is not defined at 30 R_E, 35 R_E and 40 R_E hence in AKM the lunar orbital radius from 45 R_E to 60.336 R_E is the permissible range of analysis [54].

S6.2. Methodology of theoretical formalism of LOD curve in AKM (in the main text)

$$(N)^2 \times a^3 = X^2 + \left(F \times \sqrt{1-e^2}\right)^2 \times \left(a^2\right)^2 + G^2 + 2(F \times \sqrt{1-e^2} \times a^2)(G)\{\sqrt{1-D^2}\sqrt{1-A^2} - AD\} + 2 \times X \times \sqrt{\left(F \times \sqrt{1-e^2} \times a^2\right)^2 + G^2 + 2\left(F \times \sqrt{1-e^2} \times a^2\right)G\left\{\sqrt{1-D^2}\sqrt{1-A^2} - \mathrm{AD}\right\}} \times \left\{\sqrt{1-D^2}\sqrt{1-A^2} - \mathrm{AD}\right\} \quad ..S6.39$$

Where the different symbols are defined as follows:

$$\frac{J_T}{C \times B} = N$$

Where C=present day spin moment of inertia of Earth = $0.3308 \times M_{Earth} \times R_{Earth}^2$

$$B = \sqrt{G(M+m)}2.00873 \times \times 10^7 \frac{m^{3/2}}{s}$$

J_T =Total vector sum of the Angular Momentums of E-M system.

$\frac{F^*}{C} = F$ and $\frac{I}{C} = G$ and $X = \frac{LOM}{LOD}$

Here I =spin moment of inertia of Moon= $0.394 \times m \times R_{Moon}^2$

$$Sin[\beta] = D \, and \, Cos[\beta] - \sqrt{1-D^2}$$

$$Sin[\alpha] = A \, and \, Cos[\alpha] = \sqrt{1-A^2}$$

$$Sin[\varphi] = B \, and \, Cos[\varphi] = \sqrt{1-B^2}$$

$$Cos[\alpha]Cos[\varphi] - Sin[\alpha]\mathrm{Sin}[\varphi] = \sqrt{1-A^2}\sqrt{1-B^2} - AB \quad ....S6.30$$

The empirical relation describing the evolution of Moon's orbital plane inclination with respect to the ecliptic is [54]:

$$Inclination angle \alpha = \frac{1.18751 \times 10^{25}}{a^3} - \frac{7.1812 \times 10^{16}}{a^2} + \frac{1.44103 \times 10^8}{a} - 8.250567342 \times 10^{-3} \quad ...S6.31$$

The empirical relation describing the evolution of Moon's obliquity angle (β) is given as below [54]:

$$Moon's Obliquity angle \beta == 3.36402 - 1.37638 \times 10^{-8} a + 1.32216 \times 10^{-17} a^2 \quad ....S6.32$$

The empirical relation describing the evolution of Moon's orbit eccentricity is [54]:

$$e = 0.210252 + 8.38285 \times 10^{-10} a - 3.23212 \times 10^{-18} a^2 \quad ....S6.33$$

$$\frac{LOM}{LOD} = \frac{\omega}{\Omega} = -12.0501 + 2.6677 \times 10^{-7} \times a - 4.27538 \times 10^{-16} \times a^2 \quad ....S4.16$$

$$\varphi = -0.732299 + 2.97166 \times 10^{-9} \times a \quad ....S4.17$$

(S6.31), (S6.32), (S6.33), (S4.16) and (S4.17) will be used to solve the quadratic equation given in (S4.20).Two roots of (S4.20) are obtained, out of which positive root is retained and will be used for analysis purpose.

We have all together 5 spatial function (S6.31),(S6.32), (S6.33), (S4.16)and(S4.17) describing the evolution of inclination angle (α), Moon's obliquity (β), eccentricity (e) of lunar orbit, LOM/LOD and Earth's obliquity (Φ) respectively through different geologic epochs. Table S6.2 gives the evolution of these parameters through past geologic epochs.

Table S6.2: Evolutionary history of ω/Ω (LOM/lOD), α (Inclination angle), β (lunar obliquity), e (eccentricity) and Φ (terrestrial obliquity).

a (× R_E)	a (× 10^8 m)	ω/Ω	α radians	β	e	Φ (rad)	Sin [Φ]
30	1.9113	23.3752	0.480685 (27.4°)	1.21635 (69.69°)	0.2524	unstable	-0.464076
35	2.22985	26.1194	0.26478 (15.17°)	0.952317 (54.56°)	0.236	unstable	-0.216896
40	2.5484	28.1147	0.168969 (9.68°)	0.71512 (40.97°)	0.214	0.0213773	0.0213757
45	2.86695	29.2938	0.124631 (7.1408°)	0.504756 (28.92°)	0.1849	0.113792 (6.51°)	0.113547
50	3.1855	29.5965	0.103801 (5.04736°)	0.321225 (18.4°)	0.1493	0.220227 (12.6°)	0.218451
55	3.50405	28.9877	0.0941394 (5.39379°)	0.164527 (9.4267°)	0.10714	0.314929 (18°)	0.309749
60	3.8226	27.4	0.0898729 (5.149°)	0.03466 (1.986°)	0.0584	0.398676 (22.84°)	0.388198
60.336	3.844	27.32	0.08971 (5.14°)	0.0268 (1.54°)	0.0549	0.409105 (23.44°)	0.397788

S6.2.1.The formalism of the velocity of recession of Moon in AKM:

$$V(a) = \frac{2K}{m*B} \times \frac{1}{a^{Q}}[Aa^{2} - Fa^{2.5} - \sqrt{a}] \times 31.5569088 \times 10^{6} \frac{m}{y} \quad ....S4.23$$

Except in AKM it is written as

$$V(a) = \frac{2K}{m*B} \times \frac{\sqrt{a}}{a^{Q}}[X - 1] \times 31.5569088 \times 10^{6} \frac{m}{y} \quad ....S6.34$$

In (S6.34) 'a' refers to the semi-major axis of the evolving Satellite. There are two unknowns: exponent 'Q' and structure constant 'K'. Therefore two unequivocal boundary conditions are required for the complete determination of the Velocity of Recession.

Equation (S6.33) gives the expression of the permissible Xin advanced Kinematic Model. That permissible X is substituted in (S6.34) for analysis purpose.

By classical E-M model Q is calculated to be Q=3.22684.

K=5.5 × 10^{42} Newton-mQ+1, Transit Time (from 3.012 × 10^{8} m to 3.844 × 10^{8} m) =2.38 Gy. This gives present epoch velocity of recession of Moon as=2.4 cm/y. .... S6.A.

In 'Fits and Bound model of E-M system:

K=8.33269 × 1042 Newton-m Q,

Transit Time (from 3.012 × 10^{8} m to3.844 × 10^{8} m) =1.57732 Gy.

This gives present epoch velocity of recession of Moon as =3.7 cm/y S6.B

So for our calculations we will retain the structure constant in (S6.B). This helps achieve correspondence with LLR result =3.7 cm/y.

Now this can be justified.

From 3 R_E to 45 R_E Moon does not have a smooth transit. In fact it is bumpy. It is chaotic, gets stuck in resonances and comes out of the resonances and gets stalled and resumes its tidal evolution. In fact Moon takes 3.267Gy to spirally expand from 3 R_E to 45 R_E in fits and stalled manner. From 45 R_E to 60.336 R_E, Moon is literally accelerated though smoothly coasts in 1.2 Gy to its present orbit. This accelerated spiral expansion results in present day velocity of recession of 3.7 cm/y.

Since Adv.KM is well defined from 45 R_E (Cassini State2) to 60.336 R_E so data set within this range only is considered.

S6.2.2. Theoretical formalism of LOD: Our basic assumption has been:

$$X = \frac{LOM}{LOD} \text{ Where } LOM = P_{ORB}(\text{E–Msystem}) \quad ....S6.37$$

$$\frac{2\pi}{B} \times a^{3/2} \quad \textit{from Kepler's third law}$$

From S6.25, reshuffling the terms we get:

$$LOD = \frac{2\pi a^{3/2}}{B} \times \frac{1}{X} \quad ....S6.38$$

Equation (S6.34) gives the expression of the permissible Xin advanced Kinematic Model. That permissible X is substituted in (S6.38) for generating Theoretical LOD curve.

S6.2.3.New features of lunar tidal evolution in AKM: In Figure S6.1, tidal evolution of Moon's orbital radius is given based on the new study of Matija Cuk et.al [1]

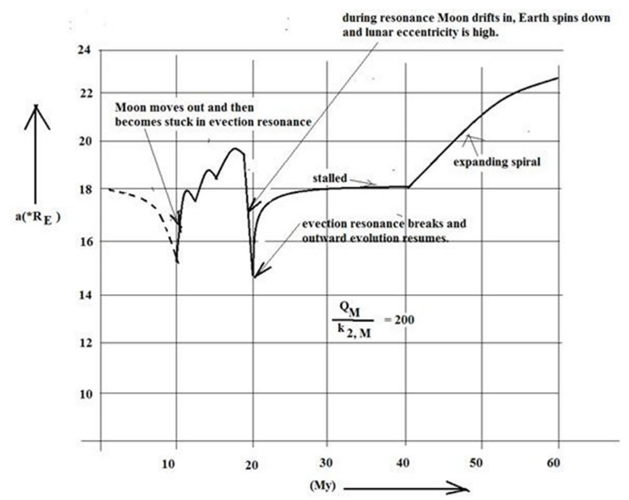

Figure S 5.1: Evolution of semi-major axis of Moon for first 60My when Laplace plane transition is encountered at 20 My and a=17 R_E.

Data Figure 5 early tidal evolution of the Moon with QE/k2, E=200 throughout the simulation in Matija Cuk, Douglas P Hamilton, Simon J Lock, Sarah T. Stewart [1]."Tidal evolution of the Moon from high obliquity, high angular momentum Earth", Nature, 539, 402-406, (2016) doi: 10/1038/nature19846]

Moon must have been formed at giant impact stage of terrestrial planets formation. In this final stage of terrestrial planet formation proto-planets collide with one another to form planets. All collisions may not lead to accretion, specifically for high velocity and/or large impact parameters. Accretion condition is derived for protoplanet collisions in terms of impact velocity, angles and masses of colliding bodies. Eiichiro Kokubo and Hidenari Genda, have adopted, realistic accretion condition in N-body simulation of terrestrial planet formation from proto-planets. In realistic accretion models about half of collisions do not lead to accretion, spin angular velocity obeys Gaussian distribution and obliquity obeys isotropic distributions independent of accretion condition.

In real life, Laplace Plane Transition plays a significant role in E-M tidal evolution due to high obliquity Earth due to giant impact. Laplace Plane shifts from Earth's equatorial plane to Solar System's ecliptic plane as Moon recedes from Earth. For any perturbed orbit, there exists a Laplace Plane around the normal of which the normal of the orbital plane of the perturbed orbit processes. The Laplace Plane undergoes a transition during lunar tidal evolution when the Moon recedes from inner region dominated by perturbation of the Earth's equatorial bulge to the region dominated by solar perturbation. At 17 R_E the shift occurs. This referred to as r_L.

$$r_L\left(Laplace\,Plane\,Transition\,orbit\,radius\right) = 2J_2\left(2J_2\frac{M_E}{M_S}R_E^2 a_E^3\left(1-e^2\right)^{3/2}\right)^{1/5}$$

....S6.39

J2=oblateness moment of Earth. As Earth spin slows down, oblateness decreases leading to r_L moving inward.

$$rL = 16 \sim 22R_E \quad ....S6.40$$

In Figure S6.1 we clearly see the interrupted and stalled tidal evolution of Moon up to 45 R_E. For Earth's obliquity Φ less than 68.9°, Laplace Plane transition is smooth and inclination and eccentricity remain zero. But for Earth's obliquity Φ greater than 68.9°, Laplace Plane transition causes orbital instability, acquires substantial eccentricity and substantial inclination driven by solar secular perturbation that operate at high inclination as seen in Kozai resonance [55].Tidal evolution of the Moon from high obliquity Earth is followed by inclination damping at the Cassini state transition due to lunar obliquity tides which(that is lunar obliquity) becomes as high as 77°periodicallyforabrief period of time.

Tides raised on the Earth by the Moon have caused an expansion of the spiral orbit. Tides raised on Moon by Earth have de-spun the Moon to synchronous rotation and driven the spin axis of Moon to a Cassini State. Cassini State is a co-processing configuration. Inco-processing configuration, Lunar's spin axis becomes coplanar with the lunar orbit normal and with the normal of the Laplace plane (which at present is coincident with the normal of the ecliptic). Moon is pushed-out due to Earth's tides but is pushed-in due to Moon's tide.

After Laplace Plane transition, Moon continues to recede and lunar spin axis passes through Cassini state transition. Regardless of the nature of the lunar rotation state, Moon's obliquity is very high during Cassini state transition and immediately following it, leading to the damping of lunar inclination. Lunar inclination is damped from 30° (obtained during Laplace plane transition) to the present value of 5.334° if we assume the long term average tidal properties for Earth and non-dissipative Moon in synchronous rotation states.

At first the Moon's orbit normal and Moon's spin axis are on the same side of the normal to the Ecliptic, indicating that the Moon is in CassiniState1.OnceCassini state is de-stabilized after some wobbling, the Moon settles in non-synchronous state somewhat similar to Cassini State 2 (with orbit normal and spin axis being on the opposite sides of the normal to the ecliptic).During this time both the inclination and obliquity (which is forced by inclination) are being damped by lunar obliquity tides. At a=35.1 R_E the Moon becomes synchronous again and enters Cassini State 2, where it stays for the rest of the simulation (this event is visible as 5° jumpin obliquity) [1].

In the "Animation of relative orientation of earth's spin and Moon's orbit during the Laplace Plane Transition" given in, the simulation covers a time span of 60 My and Moon's spiral orbit expands in fits from 10 R_E to 18 R_E [1]. Subsequently there is monotonic expansion from 18 R_E to 23 R_E.As animation progresses, Laplace Plane shifts from Earth's equatorial plane to Solar System's ecliptic plane. At 17 R_E the shift occurs.

S6.3.Theoretical validation of observed LOD for accelerated MOON: Matija Cuk et.al [1] have proposed a radically different model where Moon tidally evolves in fits and bound. Fits are due to stalling of Moon tidal evolution due to strong lunar obliquity tides created in Laplace Plane transition. Bound is due to accelerated transit time of1.2 Gy in spiralling out from 3.274 × 10^8 m to the present lunar orbit of 3.844 × 10^8 m as compared to 1.9 Gy for the classical Moon for an identical orbital radius expansion. Application of Advanced Kinematic Model to fits and bound model of Moon at ones trokere moves the tension between Lunar Laser Ranging measurement of 3.7 cm/y and theoretically predicted Lunar recession of 2.3 cm/y assuming 4.467 Gy for the classical Moon on one hand and gives a perfect match between observed LOD curve and theoretically predicted LOD curve for last 900 My and near perfect match over last 1.2 Gy with a mismatch of -1.3% [3].

6.3.1. Theoretical Formulationof LOD for last 900 My: 10 Data points given by John West Wells [6,7], and Charles P Sonnett and M A Chan [9] are considered and tabulated in Table S6.3.

Table S6.3: The history of Earth's obliquity (Φ) and Moon's orbital plane inclination (α) during Laplace Plane transition.

Time (My)	Earth's Spin(h)	Ecliptic Component Of J(%)	Laplace Plane	Earth's obliquity (Φ)	Moon's orbital plane inclination (α)	comment
0.25	2.86	153.1	Equatorial plane of Earth	70°	0°	
0.99	2.95	151.8	Equatorial plane of Earth	60°	0°	
3.4	3.21	131.8	Equatorial plane of Earth	55°	oscillatory	Falls into secular resonance
9.5	3.73	127.2	Equatorial plane of Earth	50°	oscillatory	Moon moves out and gets stuck in evection resonance
12	3.98	139	Transition	40°	oscillatory	unstable
20.5	5.66	112.1	Ecliptic	30°	oscillatory	Comes out of resonance
25						stalled
28.6	6.4	102.8	Ecliptic	20°	oscillatory	stalled
40						stalled
44.8	7.04	103.6	Ecliptic	15°	20°	Expansion resumed
59.5	7.35	103.1	ecliptic	10°	25°	expanding

Dataset given by Kaula andHarris [8] and Leschiuta and Tavella [52] have been rejected because of over-estimation errors.

List Plot of LOD for accelerated Moon for the time span of 900 My.

Figure S6.2 gives the observed LOD curve for fits and bound Moon covering a time span of 900 My.

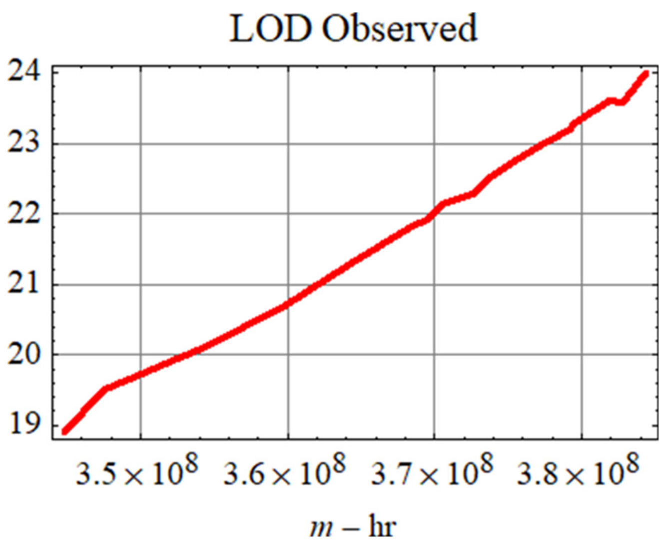

Figure S 5.2: Observed LOD curve for fits and bound Moon covering a time span of 900 My.

Generation of the theoretical LOD curve from Equation S6.26.

Equation S6.26 is as follows:

$$LOD = \frac{2\pi a^{3/2}}{B} \times \frac{1}{X} \quad \text{..... S6.26}$$

Using (S6.26) theoretical curve is generated and is displayed in Figure S6.3.

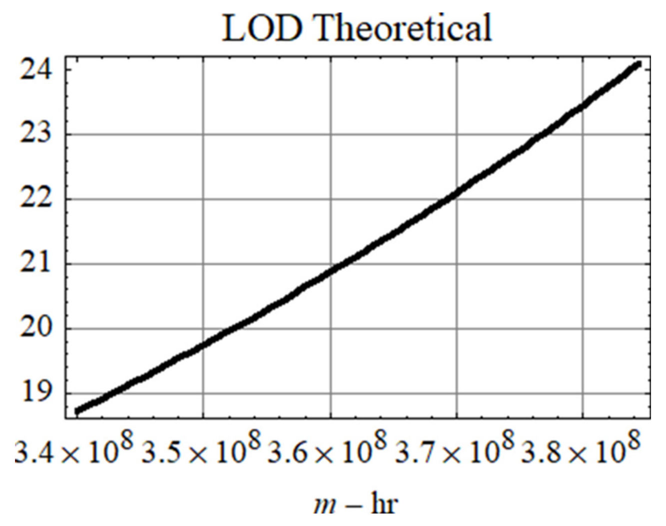

Figure S 5.3: Theoretical Plot for LOD curve for accelerated Moon over 900 My from the present.

Superposition of the Observed curve and the theoretical curve.

Superposing the two curves we get the match between theory and observation as shown in Figure S6.4.

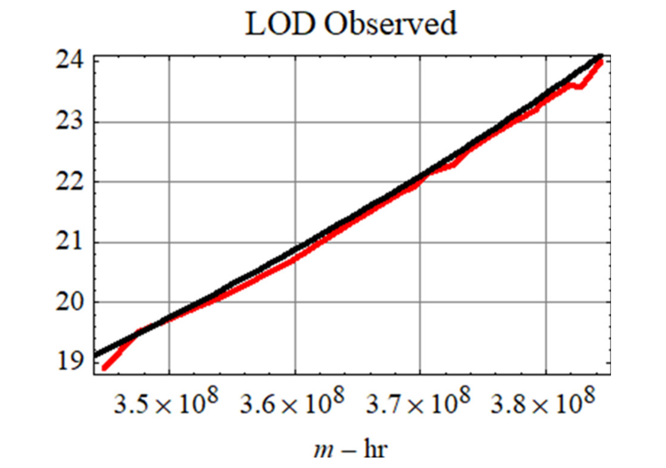

Figure S 5.4: Precise match between Theoretical and Observed LOD Plot over last 900 My.

As we see the two curves in Figure S6.4 have 100% match. Hence formalism given in S9.26 is an exact match between Observed LOD curve and theoretical LOD curve.

6.3.2. Theoretical formalism of observed LOD curve over 1.2 Gy time span, the permissible range in AKM: Validation of Observed LOD for accelerated MOON (from 3.274×10^8 m to the present orbit) using 17 Data points given by John West Wells [6,7], Kaula and Harris [8],Charles P Sonnett and Chan [9] and Leschiuta and Tavella [53] and Arbab [53].

As seen in Table S6.4, Arbab [53] provides LOD as far back as 2500 My in remote past. But his data points fall beyond the permissible range of 45 R_E to 60.336 R_E. Below 45 Ret he parameters particularly obliquity is not uniquely defined. Numerical simulation has shown that Cassini State has instability and oscillations of lunar orbital plane, hence theoretical analysis below 45 R_E has been kept out of the permissible range of AKM analysis [1].

Table S6.4: Tabulation of LOD in past geologic epochs for accelerated Moon. (Structure constant K=8.333269 N-m Q, Q=3.22684, present velocity of recession=3.7 cm/y)

Data set #	Time B.P.(years)1	Orbital radii (× 10^8m)3	LOD(h)
1	Present	3.844	24
2	45 Ma	3.8275	23.566 [8]
3	65 Ma	3.8198	23.627 [6,7]
4	135 Ma	3.79315	23.25 [6,7]
5	136 Ma	3.7927	23.2 [53]
6	180 Ma	3.7756	23 [6,7]
7	230 Ma	3.7558	22.7684 [6,7]
8	280 Ma	3.7357	22.4765 [6,7]
9	300 Ma	3.7275	22.3 [52]
10	345 Ma	3.7068	22.136 [6,7]
11	380 Ma	3.69418	21.9 [6,7]
12	405 Ma	3.6835	21.8 [6,7]
13	500 Ma	3.6422	21.27 [6,7]

14	600 Ma	3.5968	20.674, 20.7 [6,7,52]
15	715 Ma	3.5423	20.1 [53]
16	850 Ma	3.4748	19.5 [53]
17	900 Ma	3.4485	18.9, 19.2 [9,52,53]
18	1200 Ma	3.2775	17.7 [52]
19	2000 Ma	2.6(Not Permisible)	14.2 [53]
	2450 Ma (3.28 × 10^8 m)	1.96(Not Permisible)	
20	2500 Ma		12.3 [53]
21	3000 Ma		
22	3560 Ma		
23	4500 Ma		

Note: [1]Based on annual bands in coral fossils; 3Orbital radii based on accelerated Moon.

Therefore two data points of Arbab [53] have been rejected namely {2500 Ma-12.3 h} and {2000 Ma-14.2 h} have been rejected. Data points up to {1200 My ago -17.7 h} have been included in the analysis. Figure S6.5, gives the observed LOD curve over a time span of 1.2 Gy. Figure S6.6 gives the theoretical plot of LOD curve over a time span of 1.2 Gy. Figure S6.7 gives the precise match between observed and theoretical LOD curves over 1.2 Gy.

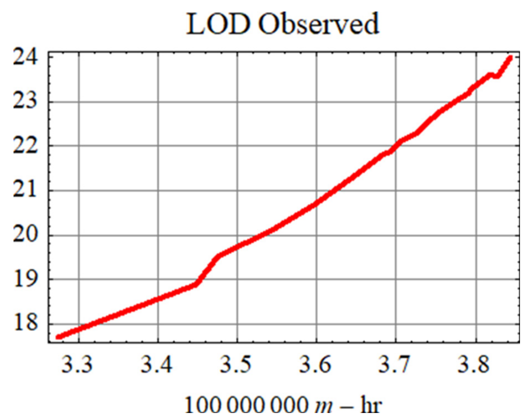

Figure S 5.5: Observed LOD curve for accelerated Moon using 17 data points covering a time span of 1.2 Gy.

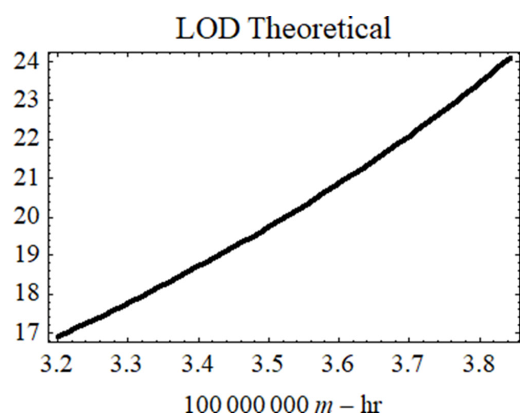

Figure S 5.6: Theoretical Plot for LOD curve for accelerated Moon covering a time span of 1.2 Gy.

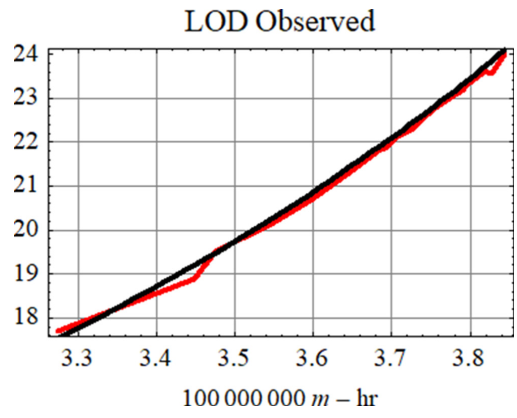

Figure S 5.7: Repeat precise match between Theoretical and Observed LOD Plot over the permissible time span 1.2 Gy and spatial range of 45 R_E to 60.336 R_E of the Advanced kinematic Model of E-M system.

As seen in superposition graph Figure S6.7 there is precise match between observed and theoretical LOD curve in the timeslot of 1.2 Gy.

For classical Moon, from 3.274 × 10^8 m to the present orbit the transit time is 1.9 Gy.

For fits and bound Moon, from 3.274 × 10^8 m to the present orbit the transit time is1.2 Gy.S6.4.

DISCUSSION

The Advanced Kinematic Model (in the main text) has been developed by including Earth's obliquity (Φ),Moon's orbital plane inclination with respect to ecliptic (α) as well as lunar obliquity (β) with respect to the lunar orbital normal and by including the vectorial summation of angular momentum vectors. The Laplace Plane transition and Cassini State transition occurring at a =(17 to 19) R_E and at 33 R_E respectively have been kept out of the permissible range of Advanced KM. Advanced KM covers the range of Moon's tidal evolution from 45 R_E to 60.335 R_E (the present orbital radius). Because of instability and unpredictability of Laplace Plane transition and Cassini State transition, the range from 3 R_E to 45 R_E has been kept out of range for Advanced KM. In classical Model of E-M system to satisfy the Age of Moon a lunar recession rate of 2.3 cm/y was being adopted which was completely distorting the time scale of tidal evolution of Moon for last 1 Gy. If lunar recession rate of 3.7 cm/y was being adopted then too short a Moon's age of 2.7 Gy was being obtained which was contrary to the observed Moon's age as obtained from Moon's rocks analysis obtained in Apollo Mission. This conundrum got resolved only after the publication of. land mark paper by Matija Cuk, Douglas P Hamilton, Simon J Lock, Sarah T Stewart [1] on Moon's tidal evolution in high obliquity, high angular momentum Earth. By adopting the Lunar Laser Ranging data of lunar recession, the AKM in one stroke became self consistent in all respects namely we obtained present Earth day of 24 h, present LOM/LOD=27.322, present lunar recession rate of 3.7 cm/y and most of all we got a precise match between observed LOD curve and theoretical LOD curve. This high obliquity, high angular momentum Earth as the origin of Moon also resolved isotopic conundrum and gave a robust mechanism for arriving at climate friendly low obliquity Earth.

S6.5. CONCLUSION

Using Advanced Kinematic Model to obtain a perfect match between observed LOD curve and theoretical LOD curve has been a crowning achievement as well as the ultimate vindication of Advanced KM. This paper has laid to rest all the nagging doubts which have been there for the empirical nature of the tidal torque developed in Kinematic Model. This paper has proved with 95% confidence level that Advanced KM is a valid model and well tested model which can be used with accuracy and reliably for analyzing two body tidally interacting systems. The application range of Advanced KM can be planet-satellite, planet hosting star and planet, star binary, Neutron star binary, neutron star-black hole binary or black hole binary. In subsequent papers the validity of advanced will be proved in this wide range of binary pairs.

Most of all the precise theoretical formalism of observed LOD curve has paved the path for searching the necessary precursors for Early Warning and Forecasting Methods (EWFM) for earthquakes and sudden volcanic eruptions.

S7. GUTENBERG-RICHTER LAW OF CHAOS

The actual sidereal day length does not secularly increase. It has periodic variations as well as non-periodic variations. If it is plotted over a secularly lengthening of day curve there will be deviations. The irregular deviations follow Gutenburg-Richter Law of chaos and hence it is chaotic and not random. This chaos implies that it has underlying causative factors. The various causative factors are plate-tectonics, ice-caps expansion and thawing, El-Nino Ocean Currents, electromagnetic coupling between core and mantle and global wind pattern interactions with various mountain ranges. If the various signatures are identified then we may isolate the precursors of Earth-quake and Sudden Volcanic Eruptions in l.o.d curve fluctuations.

It is clear that long range correlation of deviation implies chaos and chaos implies causative factors. Subduction of oceanic plates deep under the continental plates forces the folding of the Earth's crust into mountain ranges. It also causes molten magma / lava to rise through weak portions of Earth or through mid-oceanic ridges which is rupturing apart as sudden volcanic eruptions.

Apart from head-on collisions of tectonic plates the rear sideway sticking and slipping.

These lateral movement give rise to rupturing faults or premonitory creeps.

Rupturing faults behave like sand-piles during stasis. Premonitory creeps are non-critical. Gradually it develops into an universal critical class. Avalanche rupture occurs. The length of rupturing fault determines the magnitude of Earth-quake.

N (E)=1/(E)P

Where N (E) =number of Earthquake even to f size E in a given observation period. E=the energy e leased in a given Earthquake.

P=Power law =the signature of the chaos.

Plotting of the real-time sidereal day length on the theoretical curve will give a chaotic scatter and chaotic scatter should be related to geo-tectonic movements which is the underlying causative factor of Avalanche Break-down in form of Earth-Quakes or sudden volcanic eruption of dormant volcanoes. This Avalanche Breakdown is followed by long periods of stasis. The chaotic nature becomes evident if the deviations follow Gutenburg-Richter Law. Gutenburg-Richter law comes from Sand-Pile Theory [56,57].

REFERENCES

1. Ćuk M, Hamilton DP, Lock SJ, Stewart ST. Tidal evolution of the Moon from a high-obliquity, high-angular-momentum Earth. Nature. 2016;539(7629):402-406.
2. Barboni M, Boehnke P, Keller B, Kohl IE, Schoene B, Young ED, et al. Early formation of the Moon 4.51 billion years ago. Sci Advan. 2017;3(1):e1602365.
3. Dickey JO, Bender PL, Faller JE, Newhall XX, Ricklefs RL, Ries JG, et al. Lunar laser ranging: A continuing legacy of the Apollo program. Scien. 1994;265(5171):482-490.
4. Darwin GH. XIII. On the precession of a viscous spheroid, and on the remote history of the Earth. Philos Trans R Soc. 1879;170:447-538.
5. Darwin GH. XX. On the secular changes in the elements of the orbit of a satellite revolving about a tidally distorted planet. Philos Trans R Soc. 1880;171:713-891.
6. Wells JW. Coral growth and geochronometry. Nature. 1963;197:948-950.
7. Wells JW. Paleontological evidence of the rate of the Earth's rotation. Earth Moon Sys. 1966:70-81.
8. Kaula WM, Harris AW. Dynamics of lunar origin and orbital evolution. Rev Geophys. 1975;13(2):363-371.
9. Sonett CP, Chan MA. Neoproterozoic Earth-Moon dynamics: Rework of the 900 Ma Big Cottonwood Canyon tidal laminae. Geophys Res Lett. 1998;25(4):539-542.
10. Sharma BK. Theoretical Formulation of Earth-Moon System revisited. Indian Science Congress. 1995:17.
11. Sharma B, Ishwar B. Lengthening of day (lod) curve could be experiencing chaotic fluctuations with implications for earthquake predictions. COSPAR Scientific Assembly. 2002;34:3078.
12. Ida S, Canup RM, Stewart GR. Lunar accretion from an impact-generated disk. Nature. 1997;389(6649):353-357.
13. Sharma BK, Ishwar B. Planetary Satellite Dyanics: Earth-Moon, Mars-Phobos-Deimos and Pluto-Charon (Parth-I). COSPAR Scien Assem. 2004.
14. Sharma BK, Ishwar B, Rangesh N. Simulation software for the spiral trajectory of our Moon. Adv Space Res. 2009;43(3):460-466.
15. Sharma BK. The Architectural Design Rules of Solar Systems Based on the New Perspective. Ear Moon Plan. 2011;108:15-37.
16. Sharma BK. Iapetus hypothetical sub-satellite re-visited and it reveals celestial body formation process criteria in the Primary-centric Framework. COSPAR Scientific Assembly. 2012;39:1761.
17. David TJ, Hillenbrand LA, Petigura EA, Carpenter JM, Crossfield IJ, Hinkley S, et al. A Neptune-sized transiting planet closely orbiting a 5–10-million-year-old star. Nature. 2016;534(7609):658-661.
18. Sharma BK. Theoretical Formulation of the Phobos, Moon of Mars Rate of Altitudinal Loss. J Ear Environ Sci Res. 2023;5(2):1-6.
19. Sharma BK. Comparative Study of Tidal Evolution of Mars-Phobos-Deimos Based on Kinematic Model and Based on Seismic Model. J Ear Environ Sci Res. 2023;5(4): 1-12.

20. Wang H, Weiss BP, Bai XN, Downey BG, Wang J, Wang J, et al. Lifetime of the solar nebula constrained by meteorite paleomagnetism. Science. 2017;355(6325):623-627.

21. Stephenson FR, Houlden MA. Atlas of Historical Eclipse Maps: East Asia 1500 BC-AD 1900. Cambri Univer Press. 1986.

22. Stephenson FR. Historical eclipses and Earth's rotation. Astron Geophys. 2003;44(2): 2.22-2.27.

23. Morrison LV. Tidal Deceleration of the Earth's Rotation Deduced from Astronomical Observations in the Period A D. 1600 to the Present. Tidal Frict Earth's Rotat. 1978:22-27.

24. de Jong T, van Soldt WH. The earliest known solar eclipse record redated. Nature. 1989;338(6212):238-240.

25. Love AE. Some Problems of Geodynamics: Being an Essay to which the Adams Prize in the University of Cambridge was Adjudged in 1911. Univers Press. 1911.

26. Walter Heinrich MU, Macdonald GJ. The Rotation of the Earth: a Geo-physical Discussion. Cambridge Univer Press. 1960.

27. Black BA, Mittal T. The demise of Phobos and development of a Martian ring system. Nat Geosci. 2015;8(12):913-917.

28. Zahn JP. Present State of the Tidal Theory. Binaries as Tracers of Stellar Formation, Cambridge Univ. Press. Cambridge. 1992:253.

29. Zahn JP. The dynamical tide in close binaries. Astron Astrophys. 1975;41:329-344.

30. Zahn JP. Tidal friction in close binary stars. Astron Astrophys. 1977;57(3):383-394.

31. Stephenson FR, Morrison LV, Smith FT. Long-term fluctuations in the Earth's rotation: 700 BC to AD 1990. Philos Trans R Soc. 1995;351(1695):165-202.

32. Shi X, Willner K, Oberst J. Evolution of Phobos' orbit, tidal forces, dynamical topography, and related surface modification processes. Lunar Planet Sci Conferen. 2013;1719:1889.

33. Jeans JH. How the Moon will disintegrate. Nenon Practic Machin. 1936.

34. Schröder KP, Connon Smith R. Distant future of the Sun and Earth revisited. Mon Notices Royal Astron Soc. 2008;386(1):155-163.

35. Dykla JJ, Cacioppo R, Gangopadhyaya A. Gravitational slingshot. Am J Phys. 2004;72(5):619-621.

36. Jones JB. How does the slingshot effect (or gravity assist) work to change the orbit of a spacecraft?. Sci Am. 2005;293(5):116.

37. Epstein KJ. Shortcut to the slingshot effect. Am J Phys. 2005;73(4):362.

38. Cook CL. Comment on 'Gravitational Slingshot', by Dukla JJ, Cacioppo R, Gangopadhyaya A. Am J Phys. 2004;72(5):619-621. Am J Phys. 2005;73(4):363.

39. Sharma BK, Ishwar B. A new perspective on the birth and evolution of our Solar System based on Planetary-Satellite Dynamics. COSPAR Scientific Assembly. 2004;5:635.

40. Rubincam DP. Tidal friction and the early history of the Moon's orbit. J Geophys Res. 1975;80(11):1537-1548.

41. Ward WR, Canup RM. Origin of the Moon's orbital inclination from resonant disk interactions. Nature. 2000;403(6771):741-743.

42. Yin Q, Jacobsen SB, Yamashita K, Blichert-Toft J, Télouk P, Albarede F. A short timescale for terrestrial planet formation from Hf–W chronometry of meteorites. Nature. 2002;418(6901):949-952.

43. Jacobsen SB. The Hf-W isotopic system and the origin of the Earth and Moon. Annu Rev Earth Planet. Sci. 2005;33:531-570.

44. Taylor DJ, McKeegan KD, Harrison TM. Lu–Hf zircon evidence for rapid lunar differentiation. Earth Planet Sci Lett. 2009;279(3-4):157-164.

45. Touboul M, Kleine T, Bourdon B, Palme H, Wieler R. Late formation and prolonged differentiation of the Moon inferred from W isotopes in lunar metals. Nature. 2007;450(7173):1206-1209.

46. Allègre CJ, Manhès G, Göpel C. The major differentiation of the Earth at ~4.45 Ga. Earth Planet Sci Lett. 2008;267(1-2):386-398.

47. Chyba CF. Terrestrial mantle siderophiles and the lunar impact record. Icarus. 1991;92(2):217-233.

48. Bottke WF, Walker RJ, Day JM, Nesvorny D, Elkins-Tanton L. Stochastic late accretion to Earth, the Moon, and Mars. Scien. 2010;330(6010):1527-1530.

49. Becker H, Horan MF, Walker RJ, Gao S, Lorand JP, Rudnick RL. Highly siderophile element composition of the Earth's primitive upper mantle: constraints from new data on peridotite massifs and xenoliths. Geochim Cosmochim Acta. 2006;70(17):4528-4550.

50. Jacobson SA, Morbidelli A, Raymond SN, O'Brien DP, Walsh KJ, Rubie DC. Highly siderophile elements in Earth's mantle as a clock for the Moon-forming impact. Nature. 2014;508(7494):84-87.

51. Canup RM, Esposito LW. Accretion of the Moon from an impact-generated disk. Icarus. 1996;119(2):427-446.

52. Leschiutta S, Tavella P. Reckoning time, longitude and the history of the earth's rotation, using the moon. Earth Moon Relat. 2001:225-236.

53. Arbab AI. The length of the day: a cosmological perspective. Prog Phys. 2009;1(1):8-11.

54. Sharma BK. High obliquity, high Angular Momentum Earth as Moon origin revisited by Advanced Kinematic Model of Earth-Moon System. ArXiv. 2019.

55. Atobe K, Ida S. Obliquity evolution of extrasolar terrestrial planets. Icarus. 2007;188(1):1-17.

56. Buchanan M. One law to rule them all. New Sci. 1997:30-35.

57. Coontz R. Like a bolt from the Blue. New Scientist. 1998:36-40.